Royal Netherlands
Meteorological Institute
Ministry of Infrastructure and the Environment

Sensitivity analysis for model physics in Harmonie - a start towards HarmonEPS

Folmer Krikken

De Bilt, 2012 | Trainee report

Sensitivity analysis for model physics in Harmonie - a start towards HarmonEPS

Version 1.0

Date Oktober 2012
Status Final

Sensitivity analysis for model physics in Harmonie
– a start towards HarmonEPS -

Internship report

Author:

Folmer Krikken

Supervisors:
Wim de Rooy
Jan Barkmeijer
Reinder Ronda

October 2012

Abstract

This study is a first step towards an Ensemble Prediction System (EPS) for the numerical weather prediction model Harmonie. The aim of this research was to identify suitable parameters and settings within the physics of Harmonie to represent model uncertainty. Herein we focused on the turbulence, shallow convection and the microphysics parameterizations. A total of 18 different sensitivity analyses were performed on three case studies representing summer time episodes. Harmonie proved especially sensitive to two of the perturbations: the rain evaporation rate and the maximum cloud top of the parameterized shallow convection. Halving the rain evaporation as well as removing a maximum cloud top for the parameterized shallow convection even resulted in substantial better results as compared to observations in two out of three case studies. An other aspect that came forward is that perturbations in the mass flux scheme can grow before the initiation of precipitative convection whereas perturbations in the microphysics can only grow when microphysical processes are relevant, that is in the case of substantial precipitative convection. These findings suggest that a combination of perturbations from different parameterizations might be useful in an EPS. More research is needed on sensitivity to initial and boundary conditions and other physical parameterizations. Also, this research focused on summertime convection, whereas the different perturbations will most likely behave differently in winter time convection. Therefore a season dependent ensemble setup could be beneficial for an EPS.

Table of Contents

1. Introduction

In the continuous endeavor to better understand and forecast the weather, the KNMI (Royal Dutch Meteorological Institute) recently has got a new trick up its sleeve: Harmonie. This new convection permitting model is developed in a collaboration with the Hirlam and Aladin consortia (www.hirlam.org). The model has a high horizontal resolution of 2.5 km and can explicitly resolve deep convective processes, which makes it better suited for forecasting high-impact weather situations than its courser counterpart, Hirlam, which with a resolution of 10 km still needs a parameterization for deep convective processes. As a consequence, Hirlam strongly depends on the quality of the assumptions in its convection scheme (Kain and Fritsch, 1990). Also, because of this parameterization Hirlam cannot represent fine mesoscale convective organization.

However, models with a high enough resolution, like Harmonie, come with their own set of problems. For example, Mass et al. (2002) showed that increasing the resolution of models below 10 km improves the realism of the results, but does not necessarily improve the objectively scored accuracy of the forecast. Also, Hohenegger and Schär (2007) found that error growth rates are 10 x larger on cloud-resolving scales compared to synoptic scales, due to the difference in origin of error growth (convective instabilities in stead of baroclinic instabilities). The highly non-linear nature of convective processes gives that these cloud system resolving models (CSRM's) are very sensitivity to uncertainties in initial and boundary conditions and to model uncertainties, thus limiting its use as a deterministic forecasting tool. Consequently, for Harmonie to become of full use as an operational forecast tool, a shift is needed from a deterministic approach to a probabilistic approach. In the process of building a probabilistic environment, one can e.g. perturb the initial state, boundary conditions or model physics / dynamics in such a way that these perturbations represent the uncertainties in the model results. This is already frequently used in NWP (Leutbecher and Palmer, 2007; Lewis, 2005), but mostly in synoptic scale weather models. It is however questionable whether the perturbation techniques as e.g. singular vector (Palmer et al., 1993), which is used in the ECMWF model, also work with CSRM's because of the different origin of error growth (Hohenegger and Schär, 2007). Gebhardt et al. (2008; 2010) examined the usefulness of two different perturbation techniques on the CSRM COSMO-DE. They perturbed parameters within the physics of COSMO-DE and used different lateral boundary conditions, and found both methods recommendable as part of a future ensemble design.

This study is a start in constructing an ensemble prediction system (EPS) for Harmonie. Motivated by the findings from Gebhardt et al. (2008; 2010), the aim of this research is: *to identify suitable parameters and settings within the physics of Harmonie to represent model uncertainty*.

To be able to answer the research question which is raised above, multiple parameters / settings in the turbulence, shallow convection and microphysics scheme are changed. These perturbations are tested in three different case studies and individual simulations are evaluated against observations. Also we will explain the behavior of the different perturbations.

The CSRM Harmonie and the relevant parameterizations are discussed in section 2. A description of the different physics perturbations is presented in section 3 and the three different cases are presented in section 4. Section 5 describes the results of the sensitivity analysis, finally the discussion and conclusion are dealt with section 6 and suggestions for future work in section 7. In the appendix you can find the specific changes in the code for every perturbation and the source code to generate extra output.2. Experimental set-up and model description

2.1 Experimental set-up

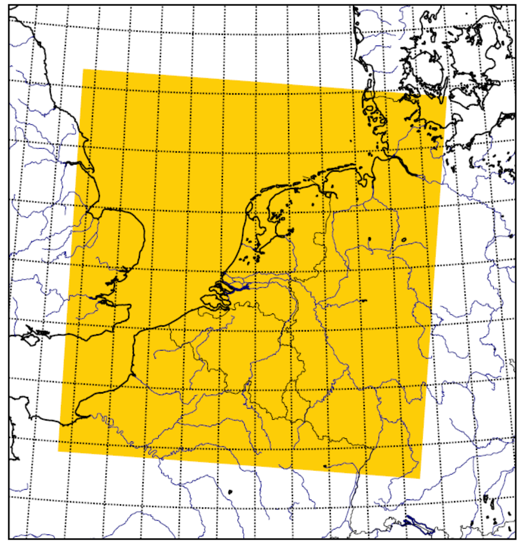

Figure 1: Location of model domain

For this research we used the mesoscale model Harmonie, cycle 36h1.4, with a single domain of 300 x 300 grid points and a grid box size of 2.5 km, centered over The Bilt, The Netherlands (fig. 1). The model has 60 vertical levels, with an increasing resolution closer to the ground (MF_60). Initial and 3 hr. boundary conditions were taken from the ECMWF. Instead of starting forecasts from the ECMWF fields, a so-called 'warm start' was done where for the initial conditions a 48 hour data assimilation prior was performed. All simulations started on 00 UTC and had a forecast length of 36 hours.
Table 1 gives an overview of the different simulations

2.2 Model description

Harmonie is a numerical weather prediction (NWP) model in the mesoscale range. It is a non-hydrostatic model with a resolution of 2.5 km and a temporal resolution of 60 seconds. Because of this high resolution the model is capable of solving the deep convective processes explicitly. Harmonie is developed within the Hirlam and Aladin consortia with the aim to improve the forecasts of severe weather phenomena and as a research tool. The physics of Harmonie is mainly adopted from the AROME model (Seity et al. 2011) while the dynamical core is taken from ALADIN-NH (Bubnovà et al. 1995). This research mainly focuses on the physics, therefore in the next section we describe that in more detail.

2.2.1 Microphysics

The microphysics are treated by the ICE3-scheme (Pinty and Jabouille, 1998). It is coupled to a Kessler scheme (Kessler, 1969) for the warm processes. The scheme handles five prognostic variables: rain (q_r) and cloud droplets (q_c) as warm processes, and ice crystals (q_i), snow (q_s) and graupel (q_g) as cold processes. The number concentrations of these variables are prescribed (single-moment scheme) and the diameter spectrum of each water species is assumed to follow a generalized Gamma distribution, which is further simplified in a classical exponential distribution. The scheme also has a subgrid condensation scheme. This allows for a small cloud fraction in non saturated environments, based on the variance of the departure from saturation inside the grid box which in turn is diagnosed by the turbulence and convection scheme.

2.2.2 Turbulence / Shallow convection

Within Harmonie there are two options for dealing with shallow convection (SC), that is Eddy-Diffusivity Kain-Fritsch (EDKF; Pergaud et al., 2009), which is the default version in AROME, and the Eddy-Diffusivity Mass Flux (EDMF_m; de Rooy and Siebesma, 2008; Neggers et al., 2009), which is the default version in Harmonie. The Eddy-Diffusivity (small scale turbulence) part of both schemes is exactly the same. First we will describe EDMF_m and then the differences with EDKF.
EDMF_m: The eddy-diffusivity (ED) part describes the small scale turbulence (i.e. local transport) in

Table 1: Overview of different perturbations.

	Run ID	Description modification	Default
1	REF	-	-
2	EDKF	EDKF MF-scheme	-
3	NOMF	No mass flux scheme	-
4	NOTOP	No cloud top for EDMF_m	4000 m.
5	15TOP	Cloud top at 1500 m.	4000 m.
6	ENTR_HIGH	Entr. at cloud base = 0.05 m^{-1}	Entr. = f(z, z_{lcl})
7	ENTR_LOW	Entr. at cloud base = 0.0005 m^{-1}	
8	ML x 2	Mixing length scale	-
9	ML x .5		
10	IP x 2	Interecept parameter	IP = 8 e6 m^{-4}
11	IP x .5		
12	SP x 2	Shape parameter	SP = 1
13	SP x .5		
14	NC x 3	Number concentration of cloud droplets	Nc = 300 cm^{-3}
15	NC x .33		
16	HAIL	Graupel characteristics changed to hail	-
17	SNOW	Graupel fall speed divided by 4	-
18	EVAP x 2	Rain evaporation	-
19	EVAP x .5		-

the planetary boundary layer (PBL). The mass flux (MF) part describes the strong organized updrafts in the PBL (i.e. non-local transport) in a mass flux formulation. The ED part is developed for Meso-NH by Cuxart et al. (2000). It calculates the exchange coefficients for temperature, moisture and momentum using a prognostic TKE equation and the Bougeault and Lacarrare (1989) length scale. This length scale computes the distance traveled by an upward and downward adiabatic parcel until it stops at the level where the parcel has lost all its TKE.

The mass flux (MF) part is developed by De Rooy and Siebesma (2008). It includes the dual mass flux framework developed by Neggers et al. (2009) which accounts for dry mass fluxes, moist mass fluxes and a combination of both. Lateral entrainment is a LES based function of height and LCL. The scheme uses a closure proposed by Grant (2001) which relates the mass flux at cloud base to a convective vertical velocity scale. This vertical velocity scale is a measure for the strength of the large eddy's in the PBL. Detrainment in the cloudy layer is a function of environmental humidity, buoyancy and cloud layer depth. A more detailed description can be found in de Rooy and Siebesma (2008).

EDKF: The Eddy-Diffusivity Kain-Fritsch (EDKF) is another eddy diffusivity mass flux scheme which uses the Kain-Fritsch entrainment / detrainment formulations, and is used in the operational run of Arome. It mainly differs from the EDMF_m scheme in three aspects: the number of updraft types (1), the massflux closure (2) and parameterization of entrainment and detrainment (3). As stated earlier, the ED part is the same. Hereafter I will describe the differences in more detail.

(1) EDKF assumes that in 1 gridbox either only moist updrafts, or only dry updrafts exist. This is very computational efficient, but as described by Neggers et al. (2009), this method fails to reproduce the

gradual transition to and from shallow cumulus convection. (2) The mass flux closure is a function of the surface boundary flux, an upward mixing length and a constant based on LES results (Pergaud et al., 2009) and is defined at the surface. (3) Entrainment and detrainment is treated with the Kain-Fritsch buoyancy sorting concept. The theory is that at the edge of the cloud multiple packages of air form with different ratios of cloud air and environmental air. The positively buoyant mixtures / packages entrain, whereas the negatively buoyant mixtures detrain. If the environmental air has a low / high relative humidity most of the mixtures are negatively / positively buoyant and detrain / entrain. A drawback to this method is that with decreasing humidity the entrainment also decreases (less mixtures are positively buoyant), resulting in the unphysical behavior of higher cloud tops (due to less entrainment) in dryer conditions. A more elaborate discussion on the deficiencies of the Kain-Fritsch approach and empirical and theoretical arguments for de Rooy and Siebesma (2008) can be found in de Rooy et al. (2012).

It must also be noted that the version of EDKF in Harmonie 36h1.4 contains a bug. In the transition from liquid water to ice, at the freezing level, the liquid water is removed but no ice is formed. This results in a lack of extra latent heat release and inhibiting the updraft to rise further than the freezing level.

2.2.3 Surface & Radiation

In this research we mainly focus on the microphysics and turbulence / convection, therefore the description of the Surface and Radiation parametrizations are only briefly described. A more detailed discription can be found in Seity et al. (2011).

Harmonie uses the Externalized Surface (Surfex) scheme (Le Moigne, 2009). This scheme uses different models for the different types of surface (land, towns, sea and inland waters). The ISBA parameterisation (Noilhan and Planton, 1989) for land, The TEB scheme (Masson, 2000) for towns, ECUME (Belamari and Pirani, 2007) for sea tiles and the Charnock's formulation (Charnock, 1995) is used for inland waters. Surfex computes the fluxes from the surface to the atmosphere and diagnostically computes the 2m temperature, humidity and 10m wind. For radiation the ECMWF IFS parameterization is used.

3. Physics perturbations

This section describes the chosen perturbations to the physics of Harmonie, why these were chosen and the expected influence of the different perturbations.

3.1 Changes in the shallow cumulus scheme

3.1.1. Maximum cloud depth

The transition from shallow to deep convection in EDMF_m is determined by the cloud depth. The assumption is that if a cloud depth reaches 4 km the clouds become large enough to be solved explicitly by the model itself, and the mass flux from EDMF_m is turned off. This maximum cloud depth for EDMF_m can be changed to lower values (more explicit treatment of convection) and higher values (more parameterized convection). In general, if more convection is treated explicitly the mass flux scheme will not remove instabilities through shallow convection resulting in a tendency of more vigorous widespread outbursts of convection. More parameterized convection causes the mass flux scheme to partly remove the instability generally resulting in a more widespread, less vigorous area of convection and in a delay in onset of resolved convection.
In this research we reduce and increase the maximum cloud depth to 1.5 km. (15TOP) and 100 km. (NOTOP) respectively. The latter results in a mass flux scheme that is never shut down as the cloud depth never reaches the critical level. Hence the word ‘shallow’ is no longer indicative.

3.1.2. Entrainment rate

The entrainment rate of the updraft determines how much of environmental air entrains into the cloud air. Larger entrainment gives a more diluted, less buoyant cloud resulting in a lower cloud top. Smaller entrainment gives the opposite results. The entrainment rate of the updraft at cloud base is set either to the maximum allowed value of 0.05 (m^{-1})(ENTR_HIGH) or the minimum allowed value of 0.0005 (ENTR_LOW), instead of being dependent on LCL and varying between these minimum and maximum allowed values.

3.1.3. Mixing length

As described in section 2.2.2, the Eddy-Diffusivity part of the EDMF schemes uses the Bougeault and Lacarrere (1989) length scale. This length scale computes the distance traveled by an upward and downward adiabatic parcel before it is stopped at a level where it has lost all its TKE. In this research we either divide or multiply this mixing length by 2, where a larger / smaller length scale results in more / less turbulent mixing. This change can have large effects in transition zones from stable to unstable or vice versa, e.g. a quicker dissipation / formation of fog or transitions from and to stable boundary layer. Wisse and Vila-Guerau (2004) have also shown that a boundary layer scheme with more turbulent mixing resulted in more widespread precipitation, but with smaller maximum values, in a case of heavy precipitation. This because of the more efficient way of distributing moisture (lower T_d), smaller convective inhibition (CIN) and smaller CAPE.

3.1.4. EDKF

As already described in section 2.2.2, EDKF only differs in the mass flux part in comparison to EDMF_m. A bug in this version of EDKF causes the updrafts to stop at freezing level, resulting in relative low cloud depth and, as a consequence, isn't shut off because of too high cloud depth (as in EDMF_m). On forehand it is hard to predict how this un-physical behavior will affect the model results.

3.2 Changes in the microphysics scheme

3.2.1 Shape and intercept parameter of the raindrop size distribution

In the ICE-3 microphysics scheme the raindrop size distribution (DSD) is described with a generalized gamma distribution. This shape of the gamma distribution is determined by a shape parameters and intercept parameter. In ICE-3 the standard value for the shape parameter (ν) is 1 (equal to an exponential distribution), and 8.0 10^7 m^{-4} for the intercept parameter. However, as shown by Smith et al. (2009) these parameters are far from constant and vary significantly over precipitation type, rain intensity and stage of development. It is therefore interesting to include perturbation to these parameters in an ensemble setup. In this research both parameters are either halved or doubled.
Figure 2 shows how this influences the distribution, where a smaller / larger shape parameter results in a distribution weighed more towards smaller / larger rain drops, and a smaller / larger intercept parameter results in a distribution weighed towards larger / smaller rain drops.

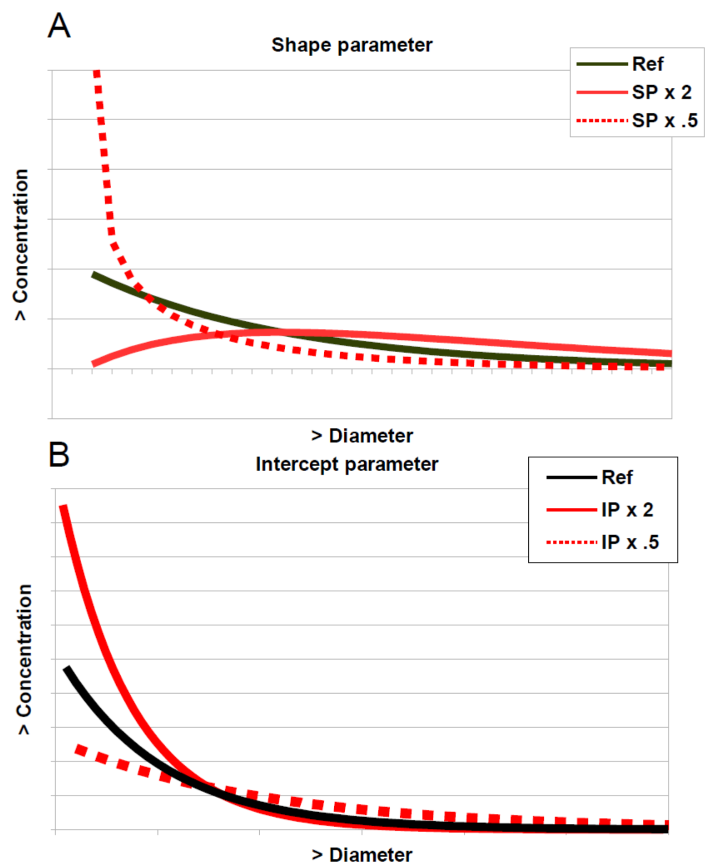

Figure 2: Raindrop size distribution for different values of shape parameter and intercept parameter.

3.2.2 Rain evaporation

The evaporation of rain is a very important process in the microphysics scheme. It affects amongst others rain rate, propagation of convection and microbursts (Knupp, 1985). It is therefore a very important variable in the non-linear behavior of convective systems. A 1st order effect of low evaporation will results in more precipitation reaching the ground, where the 2nd order effect is that the reduced outflow can result in less triggering of new convection. In contrast, a larger evaporation will results in less precipitation reaching the ground, but because of its enhanced outflow / cold pool can trigger more convection and result in more widespread precipitation.

3.2.3 Snow

This perturbation is labeled as 'snow' because the graupel fall speeds is divided by four. Therefore graupel starts to behave more like snow, as it falls much slower and it can spread over a much larger area. In this way it also has more time to melt and possibly evaporate. This removes the fast falling hydrometeor species from the microphysics scheme. Note that the characteristics of snow and graupel are still not the same. This modification produced promising results in wintertime convection (pers. comm. Sander Tijm)

3.2.4 Hail

The ICE-3 scheme only has 3 ice species, that is ice crystals, snow and graupel. In this scheme hail is assumed to behave as graupel. Richard et al. (2002) however, found that including hail (by changing the graupel characteristics to hail) significantly improved results for a simulation of a convective system over the Alps. The faster depletion of ice out of the precipitation system because of the higher fall speeds resulted in better resemblance to observations.

3.2.5. Number concentration of cloud droplets

The number concentration of cloud droplets (NCCD) prescribes the amount of cloud droplets per volume. The NCCD is closely related to the amount of condensation nuclei, therefore within ICE-3 there are different (constant) values over sea (100), land (300) and cities (900). With single-moment microphysics the constant number concentrations has always proven to be a large simplification of reality. Stevens and Seifert (2008) demonstrate the large sensitivity to NCCD in shallow cumulus, where an increase in NCCD led to a delay in the onset of rain, because the rain becomes active at higher levels. The physical reasoning herein is that more cloud droplets also need more moisture to reach the critical size to precipitate out, resulting in a delay in onset of precipitation and, generally, a decrease in precipitation amounts. Because of the large natural spread in NCCD we will divide and multiply the number concentration over land by a factor 3 (100 and 900 cm^{-3}). These values also correspond to the number concentrations used over cities (900 cm^{-3}) and over sea (100 cm^{-3}).

4. Case description

4.1. Case 1: 10 July 2010

July 10, 2010 was characterized by severe thunderstorms and heavy precipitation. A thermal low over central France triggered convection, which then moved further north because of the southerly flow. Over Belgium the multiple thunderstorms merged into a mesoscale convective system (MCS), which entered the Netherlands around 17:00 UTC. While the system moved north-eastwards a squall line formed to the south-east of the MCS. The wind gusts and thunderstorm intensity of the MCS both exceeded KNMI weather alarm criteria (> 28 ms^{-1} gusts and > 500 lightnings within 5 minutes). The MCS produced a wide band of precipitation amounting to more than 30 mm and with maximum values of 62 mm. After midnight the MCS lost strength and left the Netherlands at the North-East.

4.2. Case 2: 11 July 2010

July 11, 2010 was characterized by heavy shower over Utrecht in the afternoon, which was followed in the night by heavy convection over Groningen. The afternoon shower was a result of a slow transition of shallow convection to deep convection. The shallow convection developed over Zuid-Holland and made a transition to deep convection over Utrecht resulting in 10 mm of precipitation over a very short amount of time. The heavy convection over Groningen developed on a convergence line around midnight. It generated up to 30 mm of cumulative precipitation.

4.2. Case 3: 22 June 2008

On 22 June 2008 a cold front passed the Netherlands. Severe thunderstorms formed just ahead of this cold front and moved quickly from south-west to north-east. Within the thunderstorms large hailstones (3-5 cm.) and lightning activity of more than 500 discharges in an area of 50 x 50 km (weather alarm criteria) were observed. These thunderstorms could form because of the relative high amounts of CAPE (425 J kg^{-1} at the Bilt and 992 J kg^{-1} at Essen, Germany) and a high vertical wind shear. The large hailstones caused severe damage over eastern Netherlands and western Germany.

5. Model results

In section 5.1 I will present an overview of the model results for all three cases (case 1 in 5.1.1; case2 in 5.1.2; case3 in 5.1.3) and in section 5.2 a more in-depth discussion of interesting results that came forward in section 5.1.
The results are presented by 3 different type figures:
(1) Figure 3 (case 1), 6 (case 2) and 9 (case 3) show the cumulative precipitation for a 24h period starting and ending at 08 UTC for all 18 perturbations, the reference run (REF) and observations (OBS – rain gauge observations). In the remainder of this report precipitation stands for cumulative precipitation.
(2) Figures 4 (case 1), 7 (case 2) and 10 (case 3) show the (cumulative) precipitation spectra (5mm interval) for the different simulations and observed precipitation spectrum. Note that these graphs only include data over the Netherlands. The observations are taken from 2.5 km resolution radar observations, which are corrected to the rain gauge observations. The simulations are split over two subplots with turbulence / shallow convection in the upper plot and microphysics in the lower plot. The low precipitation amounts are also shown with a normal axis (left), instead of a logarithmic axis (right), to better distinguish differences between the simulations.
(3) Figure 5 (case 1), 8 (case 2) and 11 (case 3) show the frequency bias index (FBI, Wilks, 1995) and the equitable threat score (ETS, Schaefer, 1990). These deterministic verification scores regard precipitation as a binary event (0 for < threshold, 1 for > threshold) and are compared to the radar observations at every grid point. The data is down scaled to a resolution of 5 km, where the maximum value of the 4 involved grid points is chosen. This is done to increase the independence of the different cases (grid points). For a description of the FBI and ETS the reader is referred to appendix D.

5.1 Describing results

5.1.1 Results case 1

A first look figure 3 shows a large discrepancy between the observation and the reference run. The observations show that large parts of the Netherlands have rainfall amounts exceeding 15 mm and a large band of precipitation with more than 30 mm, with maximum value up to 62 mm. The reference run of case 1 does not show any similarity to the observations. Instead of the large band of precipitation it shows a small isolated region exceeding 15 mm and it underestimates the maximum values. Figure 4 gives similar results, where it overestimates the region with light cumulative precipitation (Fig. 4 - ref) and underestimates the region with high cumulative precipitation. The ETS (fig 5 - KER) confirms the poor performance with values around 0, indication no skill. This is a surprising result as the goal of Harmonie is to better simulate / forecast the extreme events, as this case. Note that section 5.2.1 gives a more in depth analysis of why Harmonie produces these poor results.
Even though the reference run fails to show resemblance to observations, it is still interesting to see the influence of the different model perturbations on the model simulations. Changes in the mass-flux formulation show little sensitivity, except NOTOP. The difference between 15TOP, NOMF and REF is very small, indicating the mass flux scheme isn’t very active. NOTOP does show a substantial difference compared to REF, with a larger band of precipitation in / to the east of the Netherlands, and more precipitation over central Netherlands.

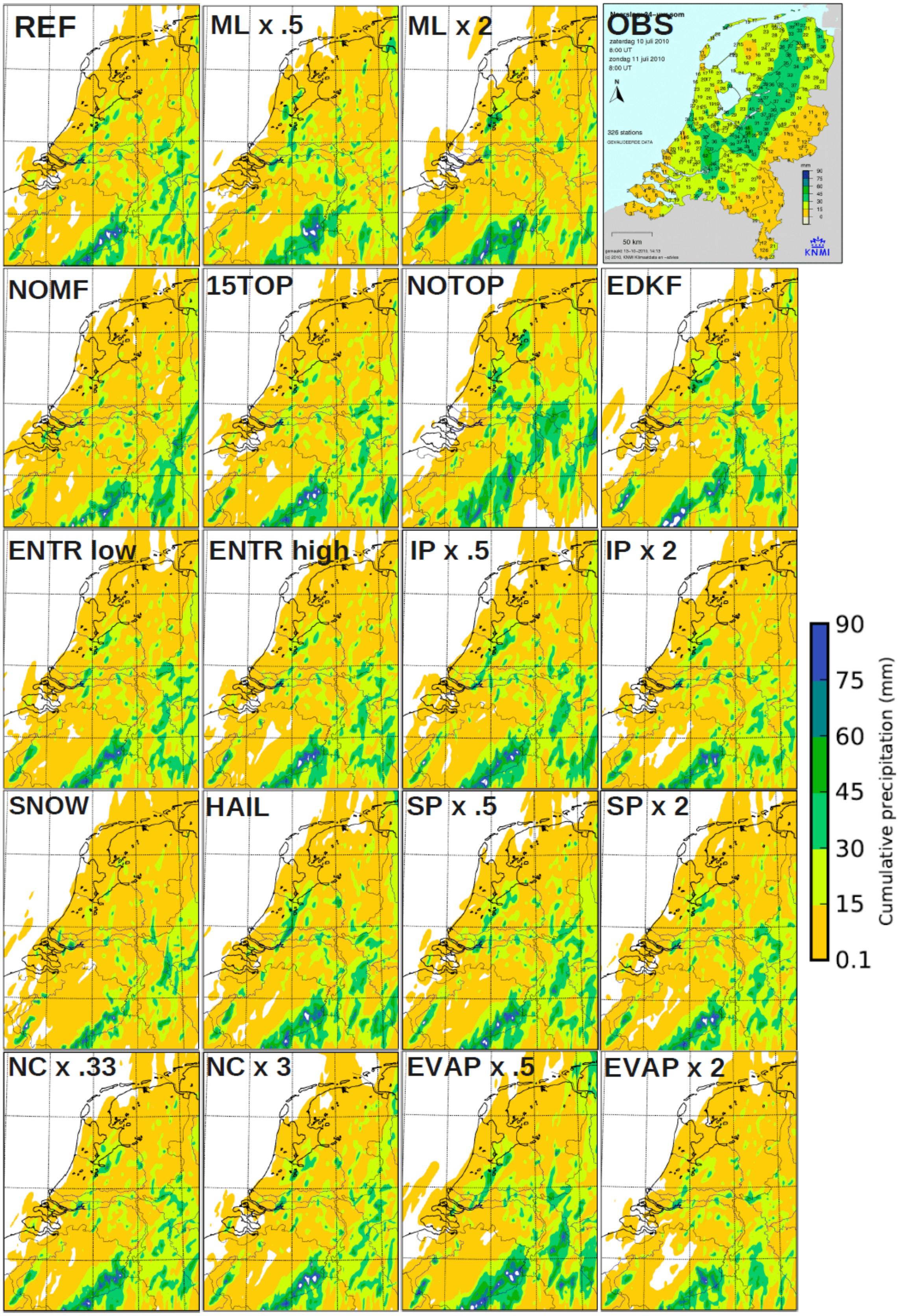

Figure 3: 24 hr Cumulative precipitation (10 July 08 UTC – 11 July 08 UTC) for OBS, REF and all 18 perturbations.

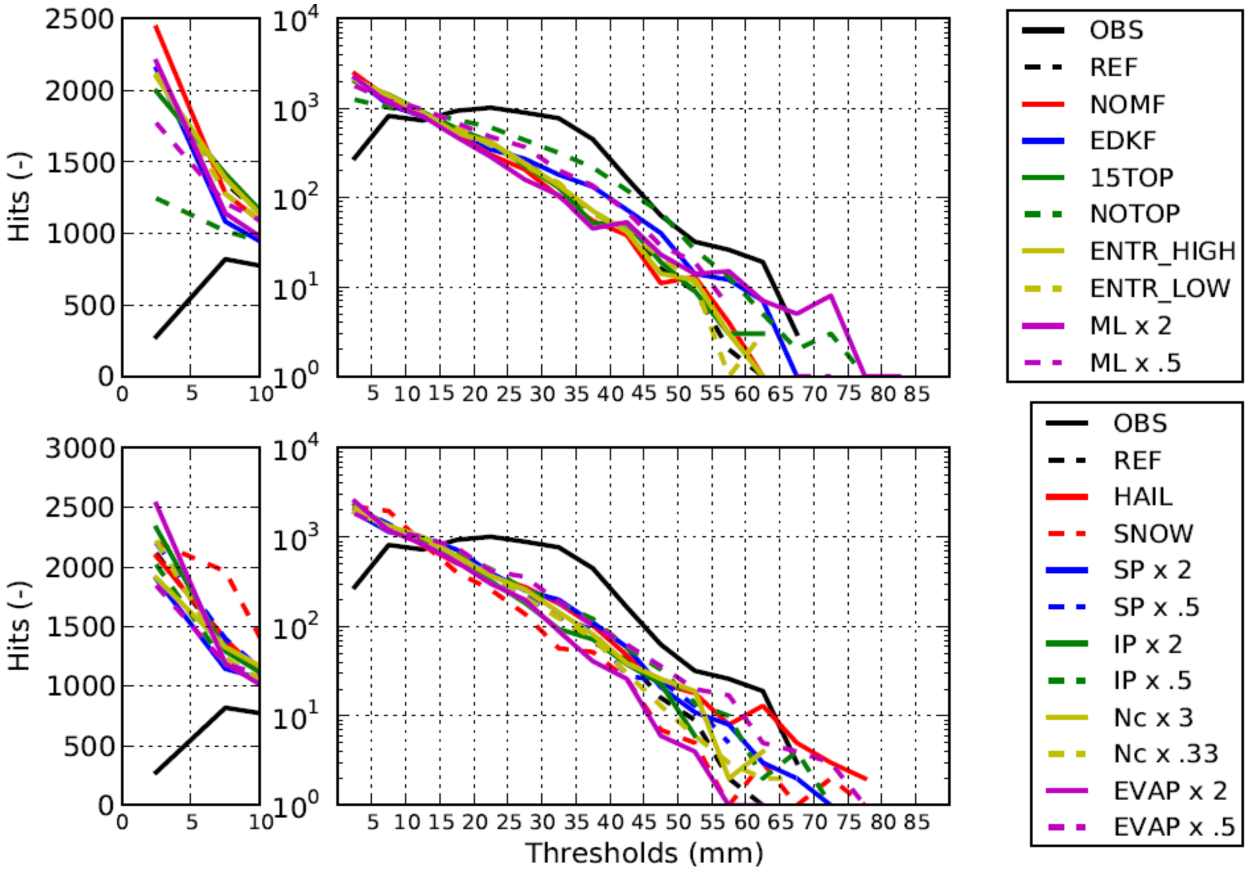

Figure 4: Spectrum of cumulative precipitation (same time period as fig. 3) with a 5 mm interval (see dotted grid) for perturbations within turbulence / shallow convection (top) and microphysics (bottom) both with a normal y-axis (left) and logarithmic y-axis (right), where the first is indicative for light precipitation amounts and the latter illustrates differences in the high precipitation amounts. Note that in this figure only data in the Netherlands is incorporated in the calculations.

In the precipitation spectrum (Fig 4) NOTOP is also closest to observations, both in the lower as higher precipitation values and in the FBI and ETS (fig. 5) it scores higher than the other simulations. This is an interesting result as one would expect that a higher maximum cloud top would yield little difference if the EDMF_m is not very active in the reference run. In section 5.2.2 we will look into this in more detail. EDKF results in a different distribution of the band of precipitation to the east of Netherlands, but further shows no large differences compared to REF. ENTR_HIGH and ENTR_LOW also show little sensitivity, but this can be expected if the mass flux scheme itself is not very active. ML x 2 and ML x .5 do have some impact on the simulation. ML x 2 results in more widespread precipitation of low values (<10 mm), as expected, but also gives higher values of precipitation (fig. 4), which is not as expected. ML x .5 results in a larger area with precipitation amounts of 15-50 mm, but lower maximum values than ML x 2. Interestingly, this is completely in contrast to our expectations (section 3.1.3), where the enhanced mixing generally leads to more widespread, but lower maximum values of precipitation. It is possible that the reduction of CIN has a larger impact than the reduction of CAPE, resulting in higher maximum values of precipitation. But then you would also expect a more widespread precipitation for ML x 2, which is not the case. It is therefore hard to physically explain these results. HAIL results in roughly the same distribution of precipitation, but the maximum values are higher (~ 10 – 20 mm, Fig 4). SNOW gives more widespread precipitation but the values are smaller, which is as expected (see section 3.2.3 for explanation). The parameters which affect the DSD do not yield large differences, except that SP x 2 and IP x .5 result in some higher values of maximum precipitation (fig. 4). This can be explained that the DSD is weighed towards larger droplets, which evaporate less quickly hence more rain reaching the surface. The influence of different NCCD (NC x 3,

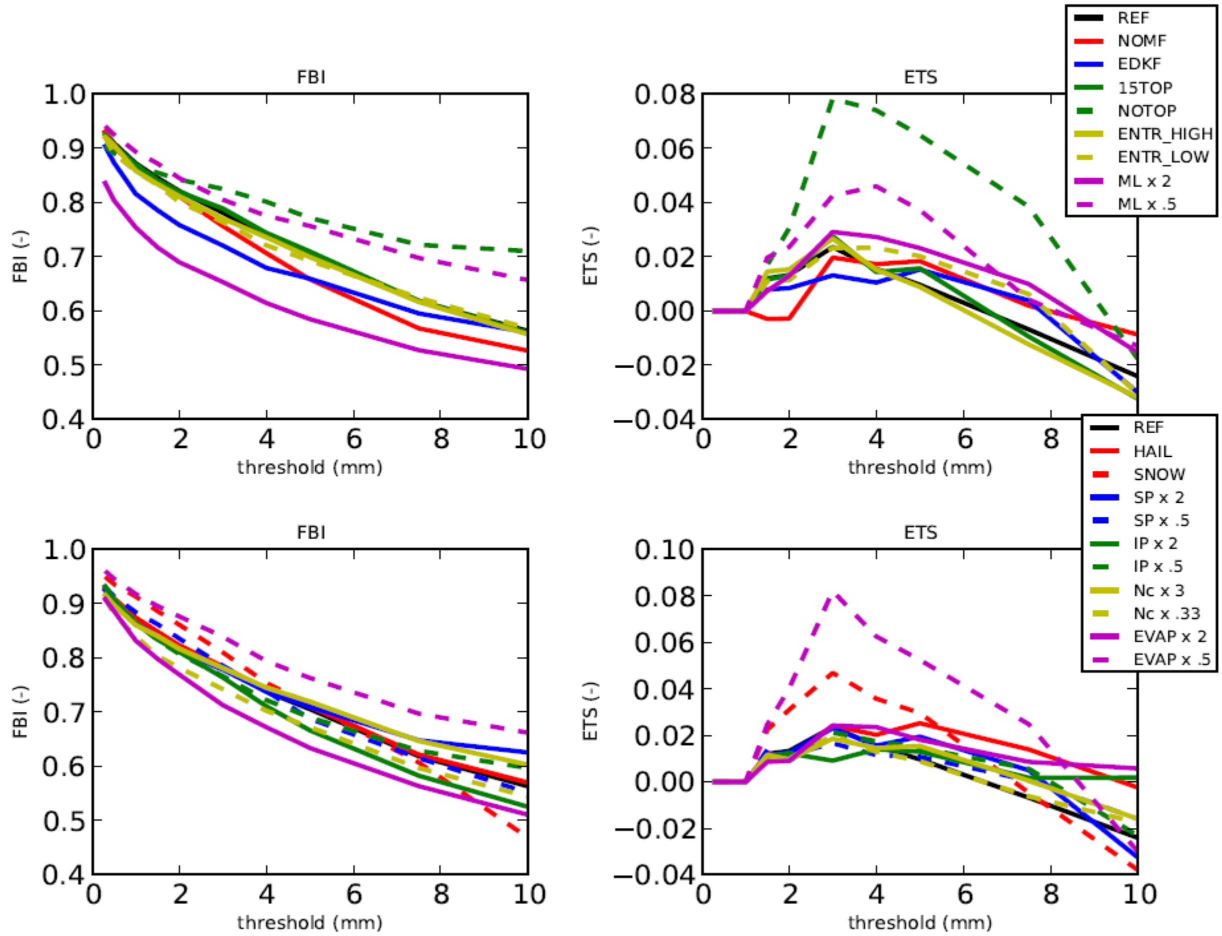

Figure 5: Frequency Bias Index (FBI) and equitable threat score (ETS) for all model simulations. The data (only over Netherlands, cumulative precipitation in same time period as fig. 3) is down scaled to 5 km resolution, where the maximum value within those grid points was taken. The perturbations in turbulence / shallow convection is shown above, the perturbations in microphysics below.

NC x .33) is little. NC x 3 results in higher precipitation amounts in north-East Belgium (thus not visible in fig. 4), which is in contrast to what is generally expected (Stevens and Seifert, 2008). But Stevens and Seifert (2008) also note that due to dynamical feedbacks a higher NC can results in larger precipitation rates, as is probably the case here. The rain evaporation yields large differences. Doubling the evaporation (EVAP x 2) results in less precipitation (both spatially as in magnitude), while EVAP x .5 results in more areas with >15 mm precipitation (fig. 4). This can of course be explained by the reduced evaporation thus more precipitation reaching the surface. The increased downdraft outflow in EVAP x 2 seems to have little effect over the Netherlands, but reduces the precipitation largely over western Germany.

5.1.2 Results case 2

Figure 6, 7 and 8 are the same figures as 3, 4 and 5 respectively, but for case 2. Reference and observations show larger resemblance to each other as compared to case 1. Apart from a band of precipitation over Overijssel / Gelderland which is not present in the observations, the reference run gives reasonable results. In the precipitation spectrum (fig. 7) OBS and REF match closely, except for the higher precipitation values, which can be attributed to the extra band of precipitation over Overijssel / Gelderland. The FBI and ETS (fig. 8) of REF also give much higher scores compared to case 1, indicating a better comparison to observations.

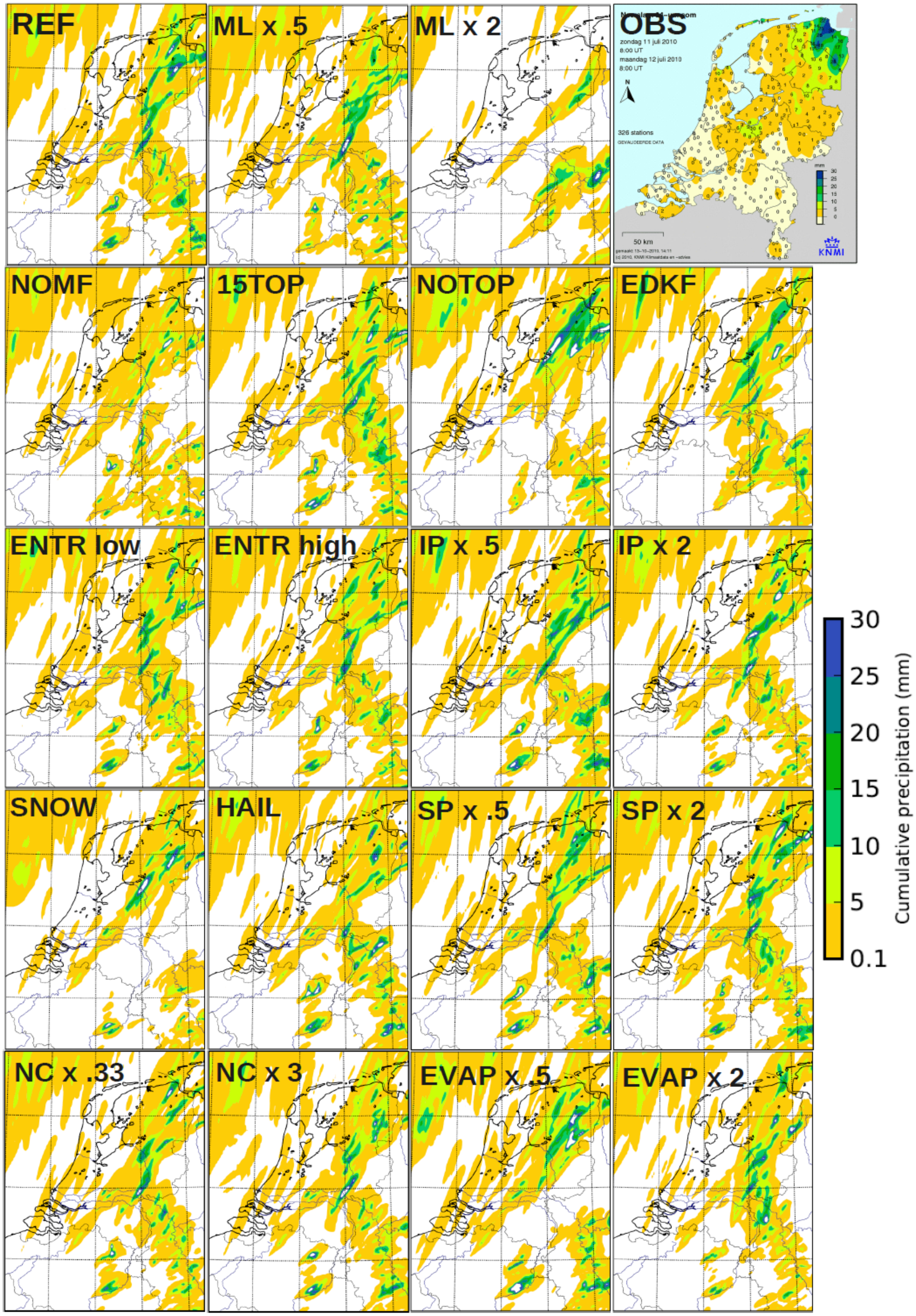

Figure 6: Same as figure 3, but for case 2.

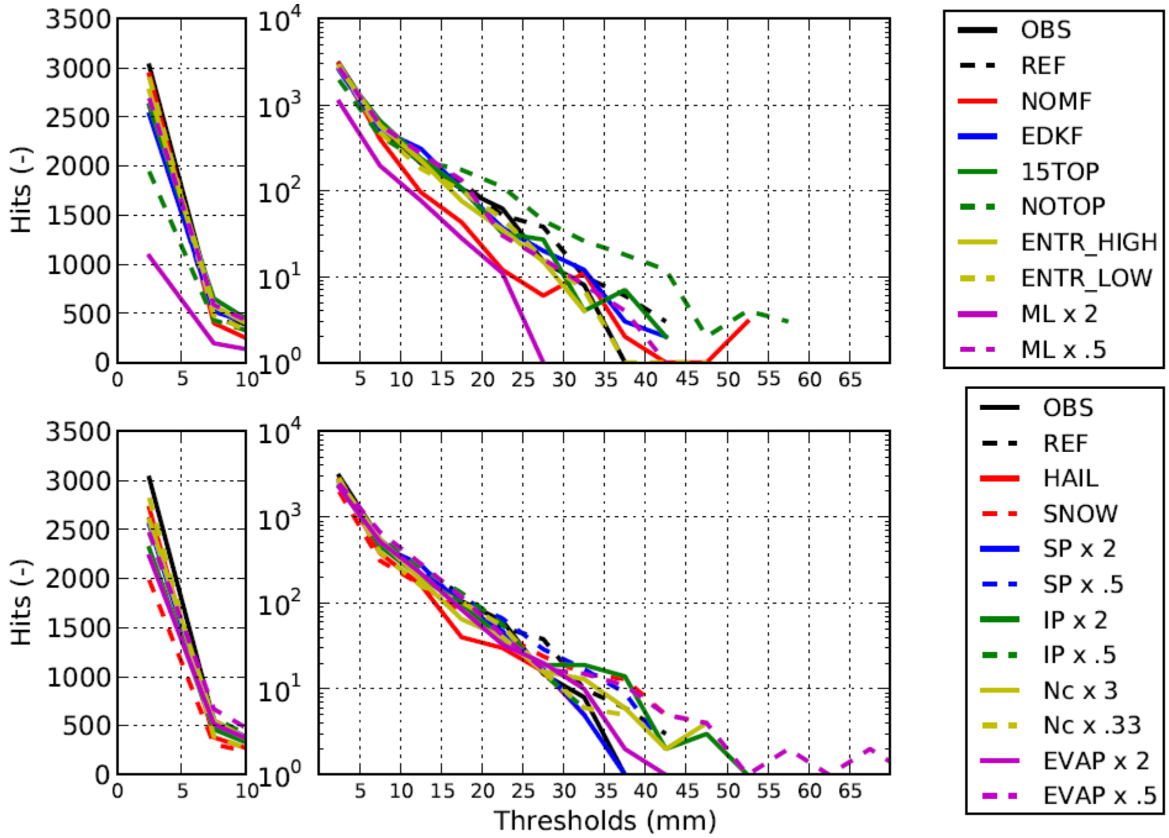

Figure 7: Same as figure 4, but for case 2.

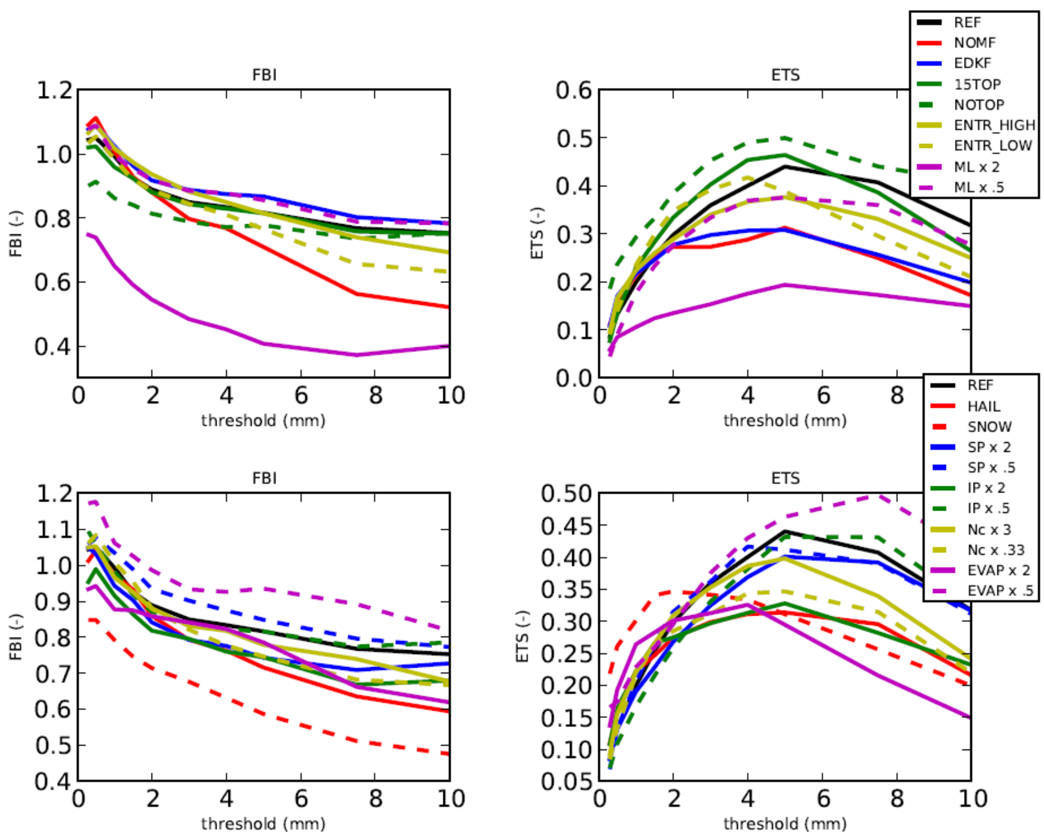

Figure 8: Same as fig. 5, but for case 2.

From figure 6 we can see that 15TOP and EDKF result in little differences as compared to REF. Also, in the precipitation spectrum (fig. 7) 15TOP, EDKF and REF give similar results. NOTOP again differs quite a lot from REF. It misses the extra band of precipitation over Gelderland (also absent in observations) and gives higher maximum values over the province Groningen. NOTOP yields the highest ETS score, but overestimates the maximum amounts of precipation (fig. 7). Generally we would expect a decrease in maximum precipitation values (see section 3.1.1), but similar to case 1 NOTOP results in higher precipitation amounts. Section 5.2.1 will explain how NOTOP can result in higher precipitation amounts. NOMF does differ from REF in this case, indicating that the mass flux part is more active as in case 1. The difference between ENTR_low and ENTR_high is a bit larger than seen in case 1, which can be expected as the mass flux scheme is more active. Interestingly, the ETS of ENTR_LOW and ENTR_HIGH are both lower compared to REF, illustrating that the default entrainment formulation in this case gives better results. Still, the sensitivity to this parameters is not very large compared to the other applied perturbations. The mixing length does have a significant influence on the results. ML x 2 results in less cumulative precipitation, both spatially as in magnitude. The scores of FBI and ETS for ML x 2 (fig.8) has by far the worst performance of all simulations of case 2.

The perturbations in the microphysics also show large differences. Reducing the falling speed of graupel (SNOW) removes the extra band of precipitation over eastern Netherlands but fails to forecast the region of high values of precipitation over Groningen and forecasts high values of precipitation at the wrong locations. This is depicted by the ETS (fig. 8), where in the lower thresholds it has a relative high score (high accuracy because it misses the band of precipitation over eastern Netherland), but in the higher thresholds it performs relatively bad (because the high amounts of precipitation are erroneously located). HAIL gives roughly the same spatial distribution of precipitation as REF, but the amounts are a bit less. The sensitivity to the DSD is dependent on the perturbation, where IP x .5 and SP x 2 (larger droplets) differs only sligthly with respect to REF (fig. 7) while IP x 2 and SP x .5 (smaller droplets) give higher maximum precipitation amounts. These results are in contrast to the outcomes of case 1. The change in number concentration (NC x .33; NC x 3) does generate some differences, but are relatively small (fig. 6). NC x 3 yields larger maximum values (fig. 7), but the spatial distribution of the precipitation is roughly the same (fig. 6). Doubling and halving the rain evaporation (EVAP) does yields large differences, where with smaller evaporation the extra band of precipitation over eastern Netherlands is absent (as in observations). A larger evaporation results in generally the same results, but with lower maximum values (fig. 7) compared to REF. Interestingly, the 2nd order effect of increasing evaporation (enhanced outflow; more triggering of convection) seems to be of large influence here as the propagation of convection is altered and the precipitation over eastern Netherlands is missing. This in contrast to case 1 where it appears the 1st order effect of enhanced evaporation, that is less precipitation reaching the surface, was of influence, especially with the reduced evaporation (fig 3 – EVAP x .5). Interestingly the ETS (fig. 8) of EVAP x 2 is the lowest, whereas the score of EVAP x .5 is the highest. In this case it is thus very important to adequately describe the evaporation of raindrops.

5.1.3 Results case 3

Figure 7, 8 and 9 are the same figures as 3, 4 and 5 respectively, but for case 3. The reference run shows quite good resemblance to observations. The maximum values are slightly underestimated and the region with higher precipitation is shifted a bit to the east. In the precipitation spectrum (fig. 8) a clear overestimation of small values and underestimation of large values is visible. This underestimation of larger values can be attributed to this shift to the east, where the higher precipitation

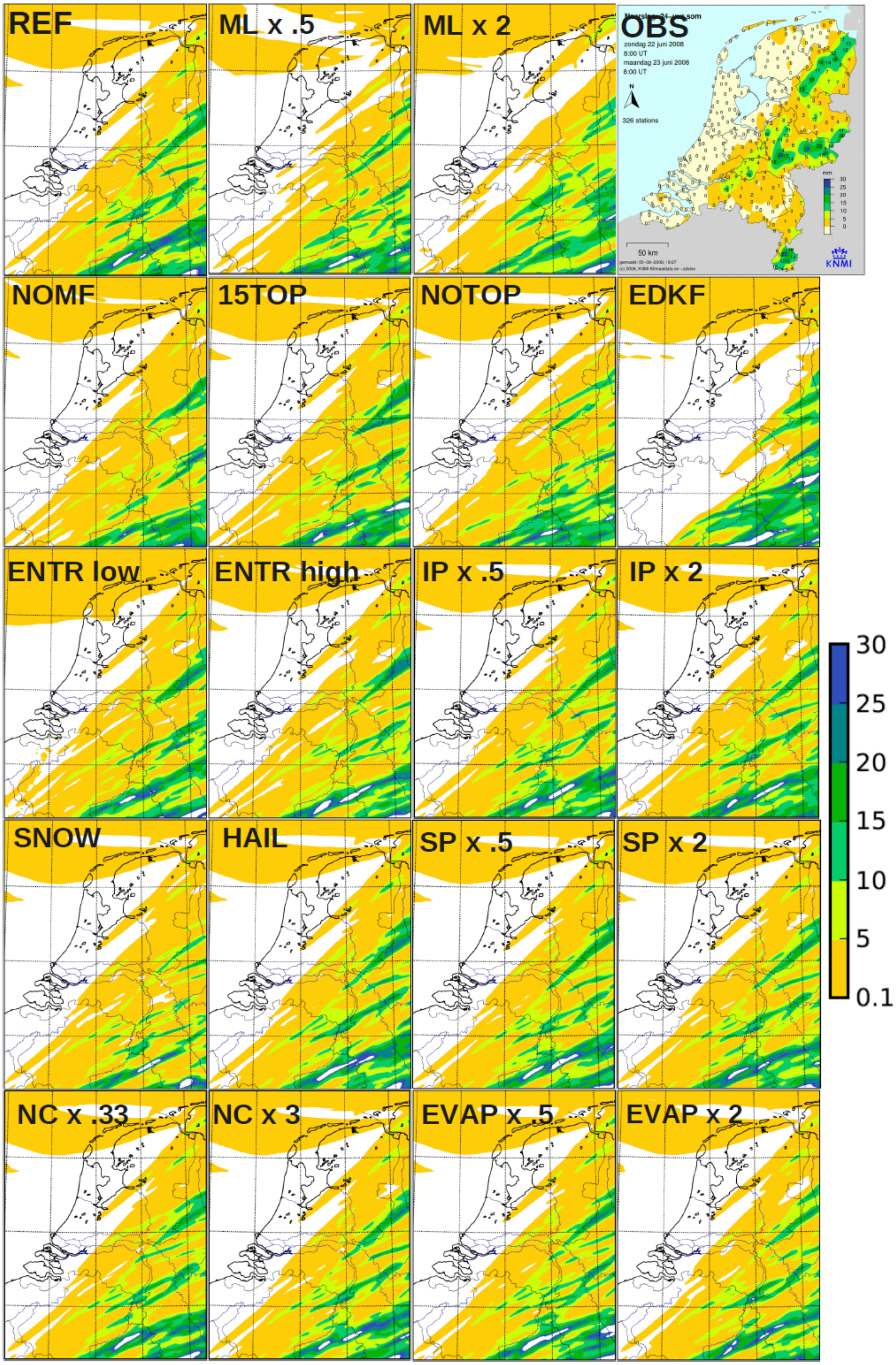

Figure 9: Same as figure 3 and 6, but for case 3.

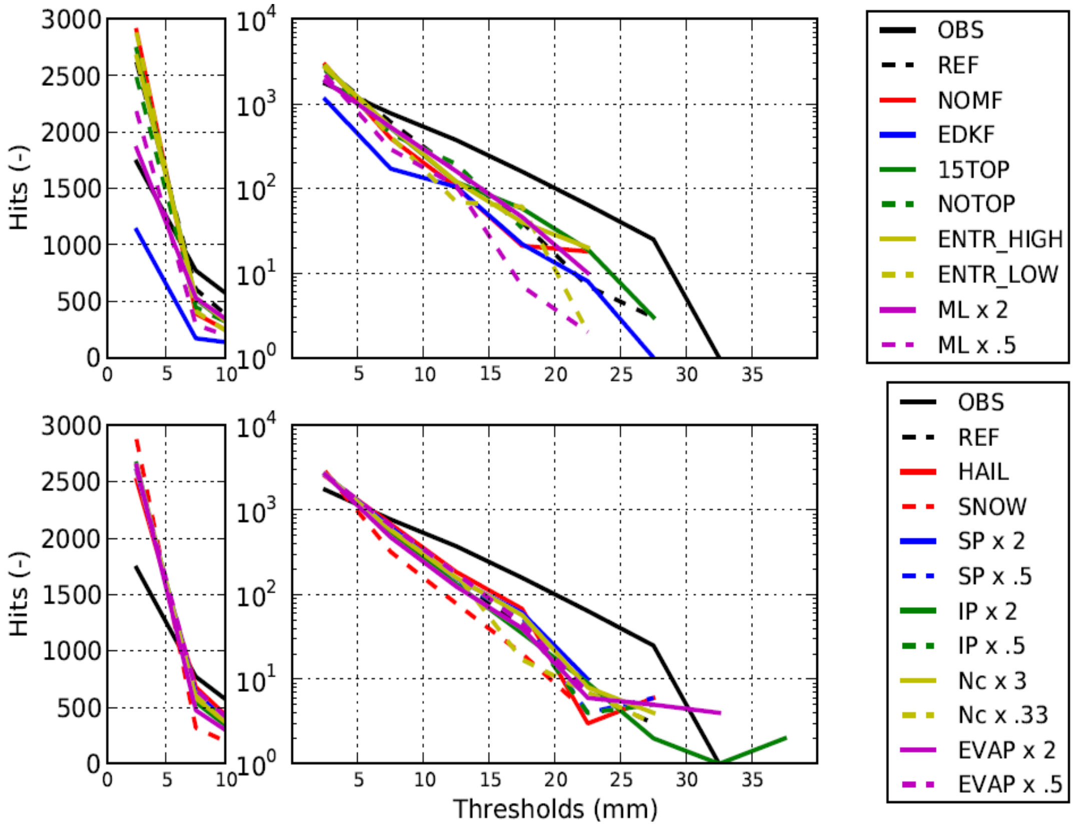

Figure 10: Same as figure 4 and 7, but for case 3.

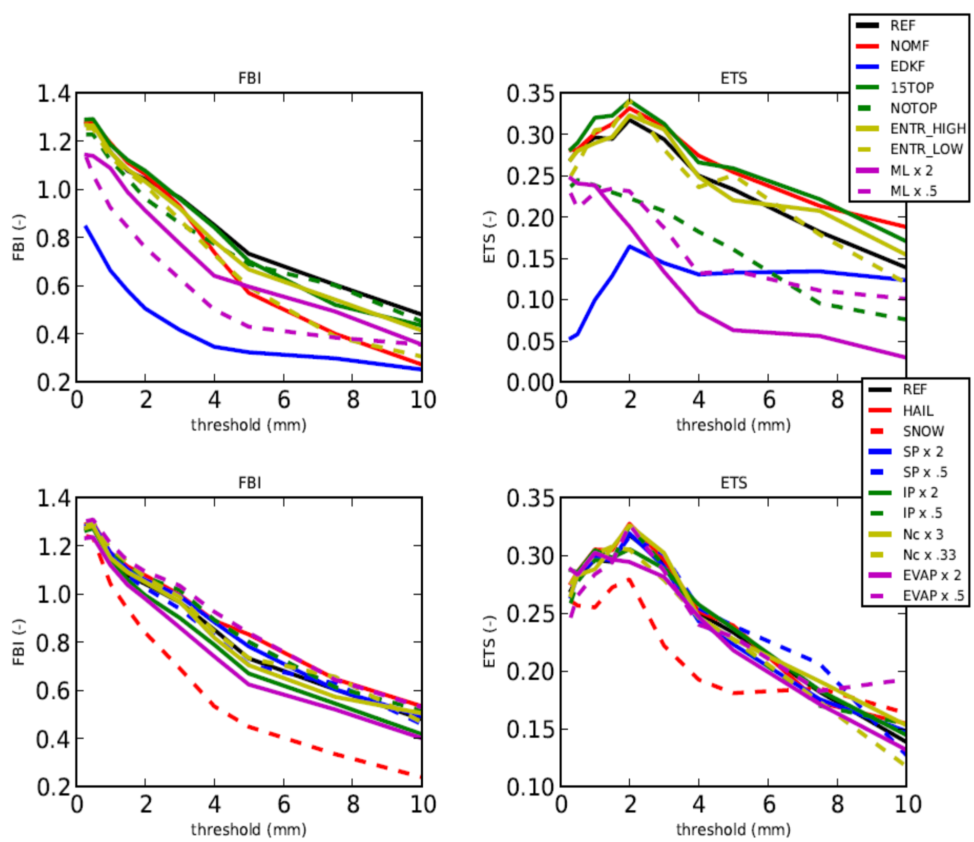

Figure 11: Same as fig 5 and fig 8, but than for case 3.

amounts are located in Germany. Since figure 8 only includes data over the Netherlands this small shift is 'punished' relatively hard in the precipitation spectrum. What can also be seen from figure 8 is the relative small sensitivity to most perturbations, compared to case 1 & 2. This mostly likely due to the dynamics of this case. Because of the high winds aloft the systems moves very fast to the north-east and, although triggered in the Netherlands, quickly moves over the eastern border. There is consequently very little time for differences between the simulations to grow. This especially accounts for the perturbations in the microphysics scheme because these differences start to grow within (deep) convective processes and not earlier as with the turbulence / shallow convection perturbations.

From the microphysics perturbations, SNOW is the only perturbation that really influences the results. The enhanced melting and evaporation because of the slower fall speed of graupel gives less precipitation (fig 8 – SNOW). The distinct behavior of SNOW is also nicely depicted by the FBI and ETS (fig. 9) of SNOW. Interestingly, a larger falling speed of graupel (HAIL) does not result in very different results compared to REF (fig. 7). Within the turbulence / shallow convection perturbations the differences are larger. Especially EDKF jumps out in all figures (7,8 and 9) because of poor results. It severely underestimates lower precipitation amounts (fig 8 -EDKF). Again ML x 2 and ML x .5 have significant influence, but both simulations give worse results (fig 9). ML x .5 results in too less precipitation, but especially ML x 2 worsens the results by not enough precipitation in the north and to much precipitation where it was not observed. This results in a poor ETS score for ML x .5, but especially for ML x 2 (fig. 9). The last simulation which really results in different results is NOTOP. Although the FBI is not very bad compared to REF (fig 9 – FBI), the ETS (accuracy of forecast) is quite bad compared to REF. This in contrast to case 1 & 2, where NOTOP improved the forecast.

5.2 Analysis

5.2.1 Surprisingly large influence of NOTOP

An interesting aspect revealed was the relative large sensitivity to NOTOP. Little sensitivity was found between NOMF and REF, indicating the mass flux part of EDMF_m is not very active. It is therefore surprising to see that NOTOP results in larger regions, and amounts, of precipitation. To investigate this, figure 12a shows the moist mass flux values (cumulative over height) of REF and NOTOP, and the

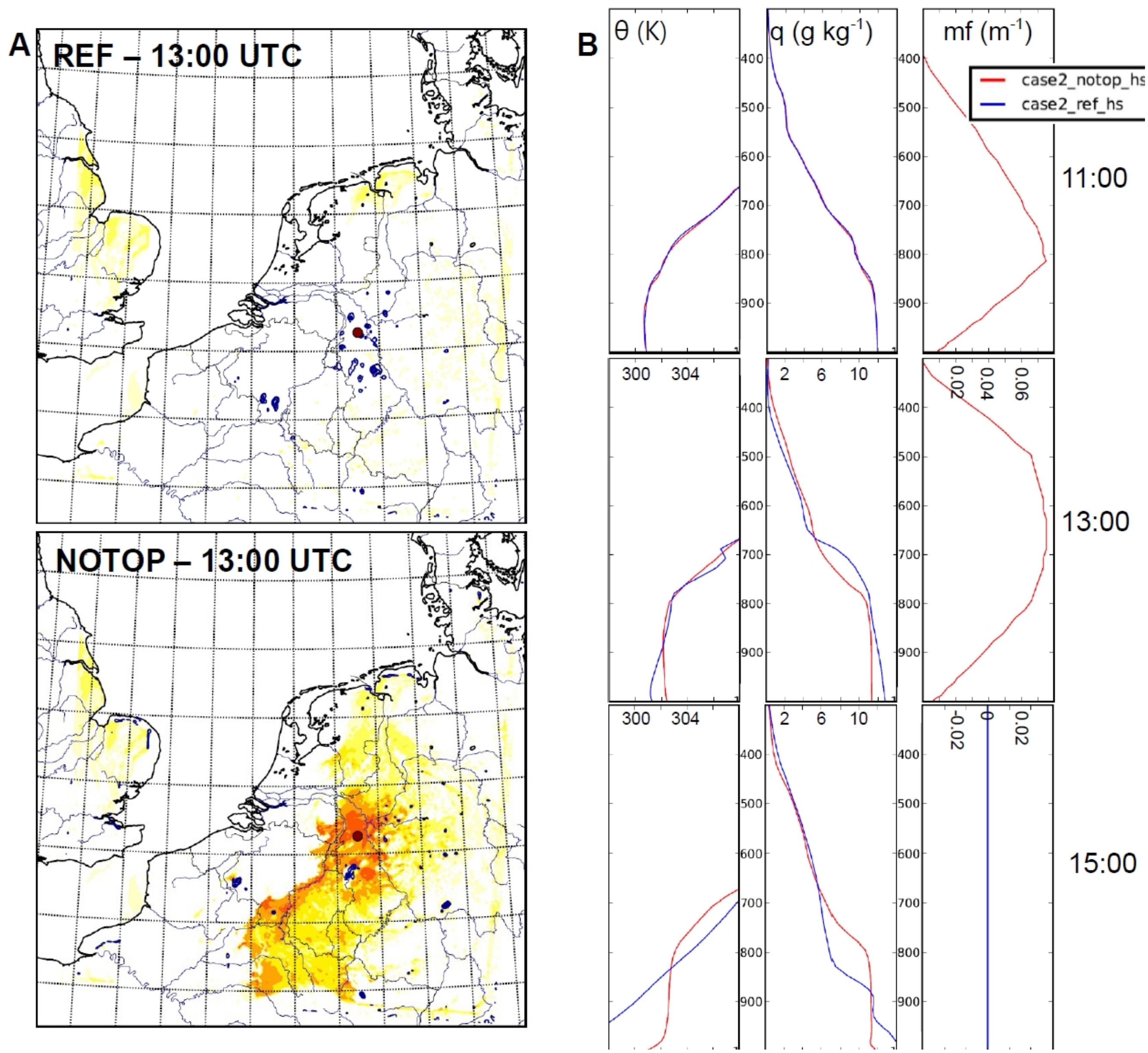

Figure 12: (A) Parameterized mass flux field (in yellow to red - cumulative over height) and the maximum vertical velocity in a column if > 1ms^{-1} (in blue - indicating resolved deep convection) for REF and NOTOP of case1, 13:00 UTC 10 July 2010. Note that because the mass flux field is cumulative over height the specific mass flux values are no longer relevant, thus absent. (B) Profiles of θ, q and mass flux on 11, 13 and 15 UTC at the location indicated with a red dot in (A) for REF (blue) and NOTOP (red).

maximum vertical velocity in a column if it is more than 1 ms^{-1} (indicating resolved convection) at 13:00 UTC. On right (fig. 12b) are the vertical profiles of potential temperature (θ), specific moisture (q) and the moist mass flux (at the location indicated with a red dot in fig. 12a) on time 11:00, 13:00 and 15:00 UTC. Figure 12a shows that NOTOP is very active over eastern Netherlands, Belgium and Luxembourg, but that in REF the mass flux scheme only shows little activity, if any. This can be explained by the maximum allowed cloud depth. Figure 12b (11:00) shows the first time the moist mass flux is active / triggered, and it immediately has a cloud top at 400 hPa. Because of this high cloud top (thus large cloud depth) only in NOTOP the moist mass flux remains active. In the beginning this results in little differences in θ and q, but over time the extra vertical transport of heat and moisture partly removes the instability. At 13:00 UTC (fig. 12b) REF shows a decrease in θ at low levels, indicating low level outflow of convection nearby. In contrast, NOTOP still parameterizes convection, and only little resolved convection is visible (fig 12a). At 15:00 UTC the θ-profile of REF is stabilized as a result of the resolved deep convection, whereas NOTOP only starts showing the first signs of downdraft outflow reducing θ at low levels. With these lower temperatures in the lower levels, the parameterized convection in NOTOP is shut off immediately. So as expected (section 3.1.1), the extra parameterized convection in NOTOP results in a delay in onset, and less widespread, resolved convection, whereas REF results in more widespread isolated burst of convection and earlier triggering of resolved convection. Because of this delay in initiation of the system in NOTOP, it interacts with a line of convection developing behind the initial convective system (not shown), in accordance with observations (not shown). Interestingly therefore, the extra precipitation over the Netherlands is a 2nd order effect of NOTOP as no convection is parameterized at the location where the extra precipitation is located. An other interesting aspect is that at locations where the mass flux scheme is active, little (parameterized) precipitation is formed (not shown). A closer look at the evaporation processes in EDMF_m reveals that roughly 1/2 of the moisture generated in the (parameterized) updraft is already evaporated before it reaches LCL, and that all moisture is evaporated before reaching the ground (not shown). This is common in shallow convection cases (RICO – Rauber et al.,2007), but very unlikely in this case where NOTOP parameterizes such deep clouds (cloud top at 300 hPa). The current evaporation of convective rain is parameterized following Kessler (1969), where evaporation is proportional to the saturation deficit and dependent on the density of rain. The constants in the formulations are tuned on the RICO (Rauber et al., 2007) shallow cumulus case. Also, it is assumed that the rain drops partly fall outside the cloud which can result in high evaporation rates above LCL. In deep convection schemes (e.g. Kain and Fritsch, 1993) it is assumed that the rain falls within the cloud, and that evaporation is only active below LCL. To test whether this would give more realistic parameterized rain reaching the surface, we changed the evaporation formulation in EMDF_m so that it only allows evaporation below LCL. Figure 13 shows the cumulative precipitation of this simulation (labeled 'NOTOP + LCL EVAP') and it is immediately clear that it much better resembles observations than REF and NOTOP (fig. 3), although it now overestimates the precipitation amounts a little. After investigating the mass flux fields and evaporation profiles (not shown), the 2nd order effect of NOTOP described

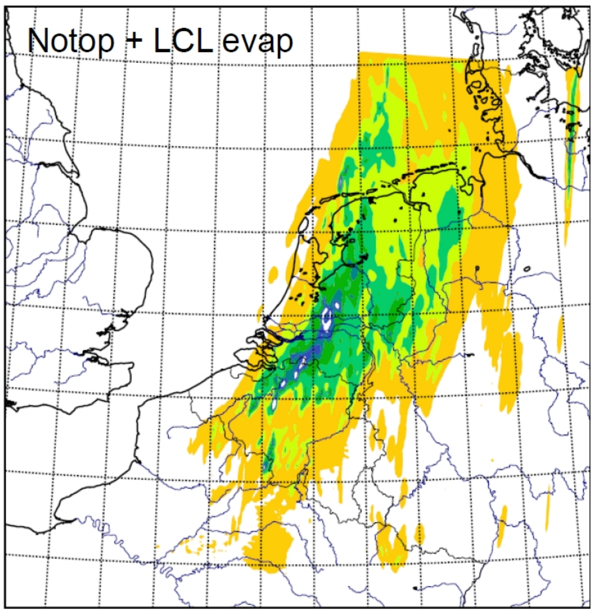

Figure 13: Cumulative precipitation of NOTOP + LCL EVAP from 08 UTC 10 July till 08 UTC 11 July 2010, Case 1.

above is even stronger in NOTOP + LCL EVAP. Although now some parameterized convective rain reaches the ground (not shown), but the most important effect is that the evaporation of convective rain is now limited to the lower levels (below LCL). This results in more evaporative cooling, thus a larger stabilizing effect of the parameterized convection.

5.2.2 *Poor performance of Harmonie in case 1*

A striking aspect which came forward from the results is the relative bad performance of Harmonie in simulating case 1. A possible explanation lies in the dynamics of this system, in combination with the relative small domain (300 x 300). The southern edge of the domain is located in northern France, but these typical summer time convective systems already initiate over central France. If these systems initiate outside of the domain of Harmonie, than the simulation is heavily dependent on the quality of the boundary conditions. Because the used boundary conditions lack microphysical data, have a 3-hour frequency and are relative course this can't be expected to give good results. Testing this hypothesis by running case 1 again with a larger domain (800 x 800) reveals that a larger domain indeed results in much better resemblance to observations (figure 13 – upper part), with a large band of precipitation stretching from the south Netherlands towards north-East Netherlands. Although the band of precipitation is located too far east, and the maximum values are overestimated, increasing the domain size still results in a large improvement. Although it would be better to use the larger domain for this complete study, this is not possible because it is computationally too expensive. We can however pick the two best simulation of case 1 (NOTOP and NOTOP + EVAP LCL) and test their influence on the larger domain. In this way we can see if the large improvements can be seen as compensating errors to the error introduced by the small domain size. Figure 14 (lower part) shows NOTOP and NOTOP + EVAP LCL. The influence of the different evaporation formulation (EVAP LCL) is not as large as with the smaller domain. Even though, the maximum values and precipitation distribution of NOTOP, especially over northern Netherlands, are in better comparison to observations (fig 3 – OBS). Allowing only parameterized rain evaporation below LCL does not improve the results as dramatically as in the smaller domain. Especially the latter can thus in this case be seen as a compensating error.

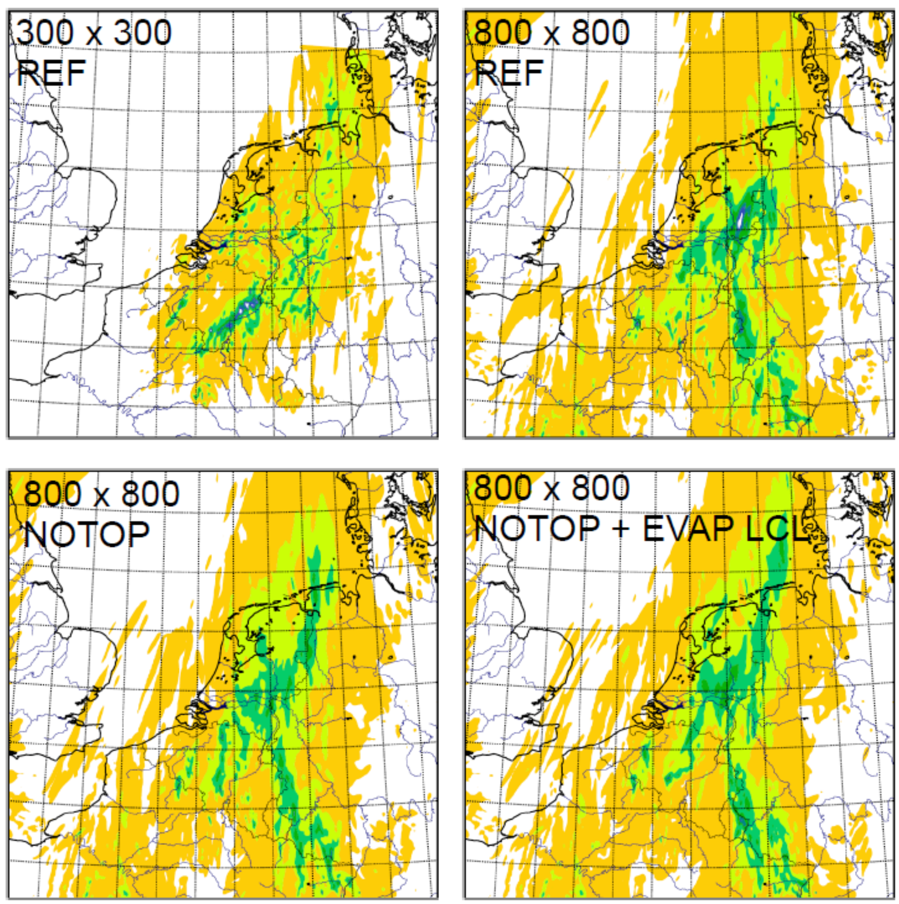

Figure 14: Cumulative precipitation from 08 UTC 10 July till 08 UTC 11 July 2010, Case 1.

5.2.3 Cold pool / rain evaporation

Because there are multiple perturbations that either directly or indirectly influence the rain evaporation, it is interesting to see how these effect the formation of cold pools. To adequately simulate mesoscale dynamics a good representation of cold pool strength is very important. As an example, if evaporation is too small, precipitation values are too large and evaporative cooling too small. As a consequence, the downdraft outflow / cold pool strength is too weak effecting the propagation of convection can change. Consequently, a different evaporation rate can completely change the system dynamics because of its 2^{nd} order effect.

Figure 15 shows the sea level pressure spectrum with a 0.5 hPa interval, ranging from 1014 to 1021.5 hPa, from the time interval between 18:00 and 22:00 UTC. This interval was chosen because the convection was most active between these times. Sea level pressure is taken instead of temperature as an indication for cold pool / downdraft outflow strength, because it is less effected by surface properties (type of soil, lakes, surface height). Pressure is affected because it rises hydrostatically due to evaporative cooling (Knievel and Johnson, 1998). Therefore these 'mesohighs' are a good indication of cold pool / downdraft strength.

From the perturbations in the mass flux scheme only NOTOP and MLx2 stand out. Because both do not directly influence rain evaporation, an explanation for their different pressure spectrum is not straight forward. At first glance, the spectrum of NOTOP seems to be caused by more parameterized convection resulting in less mesoscale organization (i.e. mesohighs). But, when taking into account that the influence of NOTOP was mostly of 2^{nd} order (as described in section 5.2.1) and that NOTOP is hardly active over the Netherlands in the time frame used in figure 15, that explanation is somewhat weakened. The perturbations applied to the microphysics scheme show larger differences than the perturbations involving turbulence and shallow convection. The runs that stand out are EVAP, IP and SP. Especially, as expected, the sensitivity to rain evaporation (EVAP) is large, where a small / large evaporation results in weaker / stronger mesohighs. The differences between the perturbations on the raindrop size distribution is also relatively large. Smaller droplets both evaporate quicker and because of the slower fall speeds also have a longer time-span to evaporate, thus evaporation is strongly related to the different drop size spectra. As can be seen in fig. 15, the perturbations that weigh towards small droplets (IP x 2, SP x .5) result in a higher pressure, and the perturbations that weigh towards larger droplets (IP x .5, SP x .5) result in lower pressure. Concluding, a lot of the results of SP and IP can be attributed to evaporative processes. This conclusion is confirmed by analysis of Morrison et al. (2009). The question which then raises is whether changing the size distribution is really beneficial in an ensemble set-up. It might just be easier to multiply the rain evaporation by several factors in the range between .5 and 2. As shown by Smith et al. (2009), the parameters controlling the size distribution of hydrometeors are fare from constant, both over time and space. But the question is whether changing the constants really introduces the uncertainty introduced by these parameters. Most of the perturbations in the microphysics are related to the inherent limitations of a single-moment scheme, that is; a fixed intercept parameter, shape parameters and number concentration. We can change the specific values, but are still bound to constant values of the different parameters. Within a double-moment scheme the varying aspect of these parameters is crucial in a good representation of microphysical processes (Morrison et al., 2009). For example, a DSD needs to be weighed towards large rain drops in the core of a convective system, but needs to be weighed more towards small droplets in the stratiform region. These varying aspects (both in time as in space) can not be taken into account in the current microphysics scheme, thus limiting the usefulness of changing the raindrop size distribution as long the parameters are constants (i.e. a single-moment scheme).

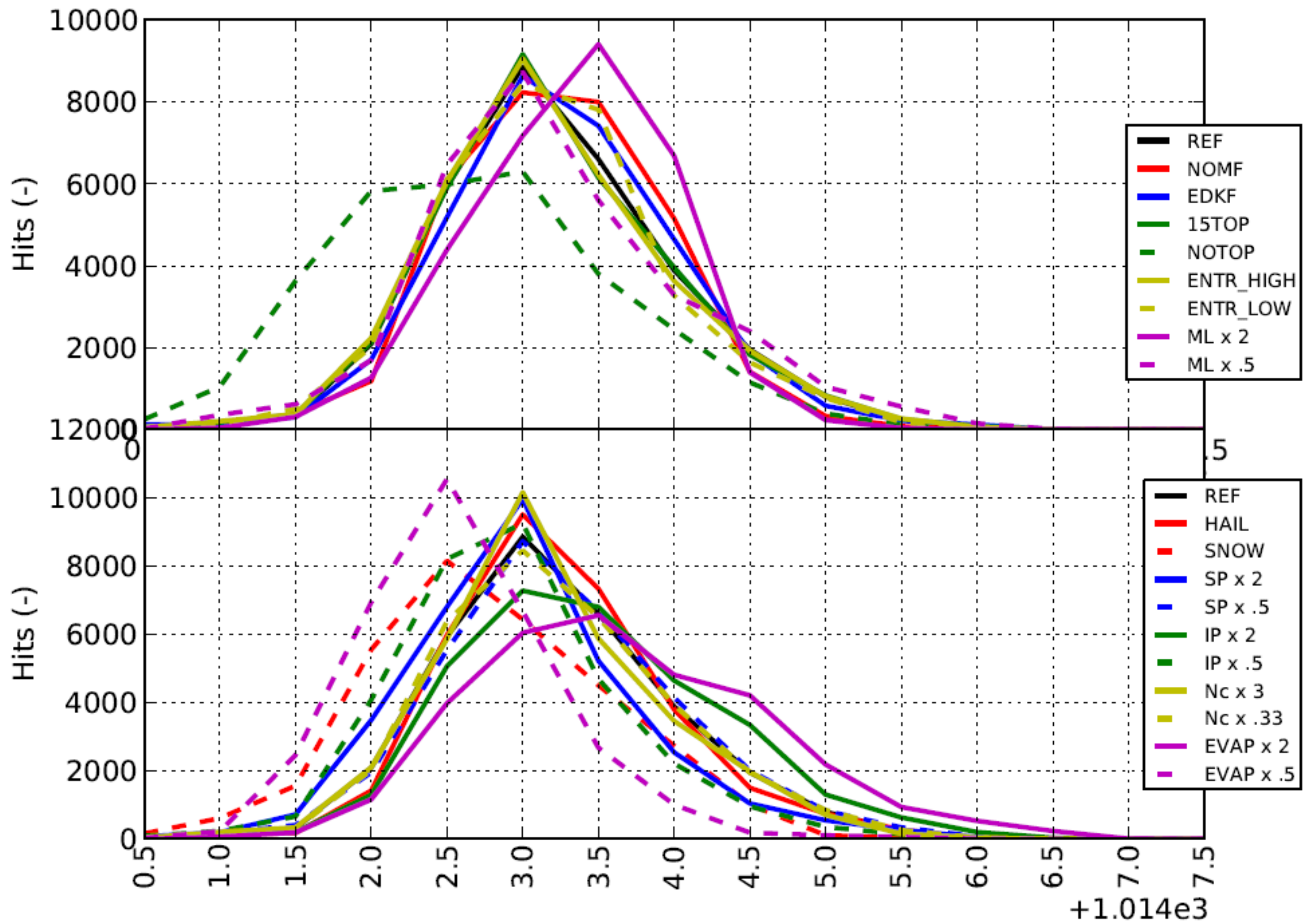

Figure 15: Spectrum of sea level pressure with a .5 hPa interval (see dotted grid) for perturbations within turbulence / shallow convection (top) and microphysics (bottom) in the time interval of 18:00 to 22:00 UTC on 10 July 2010. Note that in this figure only data in the Netherlands is incorporated in the calculations.

Although the varying aspects of the DSD parameters and evaporative processes can not be taken into account in the single-moment scheme, the results do indicate that especially reducing the rain evaporation improves the simulations (2 out of 3 cases). As describe above, a DSD needs to be weighed towards large rain drops (low evaporation) in the core of a convective system and needs to be weighed more towards small droplets (high evaporation) in the stratiform region. A single-moment scheme generally tends to overestimate evaporation in the convective core and underestimate evaporation in the stratiform region because of its (averaged) DSD (Morrison et al., 2009). When changing the evaporation both regions are affected, but apparently reducing the overestimation of evaporation in the convective core is more important than the extra evaporation in the stratiform region. So although a lower evaporation might yield more widespread (stratiform) precipitation, the storm morphology is improved by a better representation of downdraft outflow / cold pool formation.

6. Discussion and conclusions

This study is a first step towards the construction of an ensemble prediction system (EPS) for the cloud system resolving model Harmonie. The goal of this research was to identify suitable parameters / settings within the physics of Harmonie which can be employed to represent model uncertainty. We have done this by perturbing multiple parameters in the microphysics scheme (ICE-3) and the turbulence / shallow convection scheme (EDMF), and test these perturbations (18 in total) in three different cases in the Netherlands. For model evaluation we have mainly studied the cumulative precipitation as this is one of the most important output variables, and because it is very well suited for statistical analysis and comparison against observations (radar + rain gauge).
A first analysis of the quality of the forecast revealed that Harmonie had trouble adequately simulating case 1 because the domain was relatively small. A simulation with a larger domain improved the results considerably, but because these runs are very computational intensive the sensitivity analysis is done using a small domain. A consequence of this is that it is difficult to access the quality of the different perturbations. This is illustrated by the simulation with no maximum cloud top and only evaporation below LCL (within EDMF_m), where in the smaller domain significantly improves the results but in the larger domain the sensitivity is limited.
Overall, the sensitivity to the different perturbations varied widely. Doubling and halving the mixing length gave the least realistic results, where especially doubling resulted in consistently worse results. The model turned out to be very sensitive to the maximum cloud depth of the shallow convection parameterization. No maximum cloud top and thus more parameterized convection, gave in two of the three cases significant better results as compared to the reference run. EDKF mainly resulted in worse forecasts, but this might be explained by the bug which is still present in this version of EDKF. Changes in the (rain)drop size distribution (DSD) showed some sensitivity, but not very much. The number concentration of cloud droplets resulted in the smallest sensitivity of all microphysics perturbations and changes to the characteristics of the hydrometeors gives large sensitivity, especially when reducing the fall speed of graupel. Concerning the microphysics, the model is most sensitive to directly doubling / halving the rain evaporation. Halving the rain evaporation gave even better results compared to reference in two of the three cases. Concluding, the model is especially sensitive to rain evaporation and the cloud top for 'shallow' convection (more or less parameterized convection).
An interesting aspect revealed was that the different perturbations in the mass flux scheme can grow before the initiation of precipitative convection whereas perturbations in the microphysics can only grow when microphysics are relevant, that is in the case of substantial precipitative convection. Thus, to be able to cover the largest amount of model uncertainty with as little members as possible, a combination of perturbations in both part of the schemes might be useful.
For many of the perturbations a rather simple 'multiply and divide by 2' method was used for the sensitivity analysis. Although these values lie in most cases within the natural spread of the used parameter, it is still a very rough estimate of the uncertainty introduced by these parameters. For a first-guess of the sensitivity to the different parameters it provided useful, but further research is needed to better judge the applicability of the multiplication factors.

7. Suggestions for future work

(1) Uncertainties in NWP are caused by the initial state of the model, the boundary conditions and model formulations. Without looking at all three sources of uncertainties, it is hard to judge the spread generated by the perturbations in the model physics. Therefore future work also needs to implement the uncertainties of initial and boundary conditions.
(2) A more in-depth analysis is needed to investigate the specific influence of the different perturbations and to further strengthen the drawn conclusions.
(3) Due to time constrains we only looked at the microphysics and turbulence / shallow convection. For future work it is recommended to look at suitable parameters / settings within the radiation and surface scheme (Surfex), as these might represent a substantial part of the model uncertainties.
(4) All 3 cases in this research where in the summer. It would be interesting to test the different perturbations also in winter cases. Especially the changes in the microphysics will results differently because of the shift to different hydrometeors. The sensitivity to DSD was only on the raindrops, whereas in wintertime the role of raindrops diminishes. This also illustrates that some perturbations could work really well in summertime, but show no sensitivity in wintertime. If you then want to get the maximum amount of (realistic) spread between the members, with the least members possible (computational efficient), different perturbations (ensemble set-ups) are needed for the different seasons or summer- / wintertime.
(5) Combining perturbations from different parts of the model (e.g. mass flux and microphysics) can help improve the spread of an ensemble because they are active in different regions / times in the simulations. Perturbations in the mass flux scheme can grow before the initiation of precipitative convection whereas perturbations in the microphysics can only grow when microphysics are relevant, that is in the case of substantial precipitative convection.

8. Acknowledgments

I would like to thank both supervisors, Wim de Rooy and Jan Barkmeijer, for the support and constructive feedback during my internship. Furthermore I would like to thank Sander Tijm for the useful feedback on model results, Emiel van der Plas for the support on the Python language and Maurice Schmeits for the support on the statistical analysis.

9. Appendix

Appendix A

Extra output

In this section I will explain how to get more variables from the EDMF_m scheme as output, as e.g. cloud depth, mass flux type, LCL, moist mass flux, dry mass flux. The variables can be both 2D as 3D fields.

For EDMF_m most variables can be found in the routines *vdfparcelhl.F90*, *vdfhghtnhl.F90* and *vdfhghthl.F90* (located in *src/arp/phys_dmn/*). In this description I will use the LCL of the moist updraft (*ZPLCL*) as an example. This 2D field is calculated in vdfparcelhl.F90, and is further used in vdfhghtnhl.F90. The variable is already in the argument list in vdfhghtnhl.F90, therefore it only needs to be fed trough to *vdfhghthl.F90*, *apl_arome.F90* and *mf_phys.F90*. To feed it through the variable (ZPLCL) needs to be put in the argument list and be declared as a global variable. Note that ZPLCL contains the LCL of every updraft type. Because there are three updraft types it also needs to be declared as a 2D array [e.g. REAL(KIND=JPRB)   ,INTENT(OUT) :: ZZPLCL(KLON,3)].

The next step is to set up a GFL array.
In src/arp/module/yomgfl.F90 a new GFL array (here GFLMICHOU) is set up by adding the line 'REAL(KIND=JPRB),ALLOCATABLE :: GFLMICHOU (:,:,:,:)' after the other GFL arrays.
In src/arp/setup/susc2b.F90 add after the 'IF(YGFL%NDIM > 0) THEN' statement the following lines in section 4.2:

```
ALLOCATE(GFLMICHOU(NPROMA,NFLEVG,3,NGPBLKS))
IF (LLP) WRITE(IU,9) 'GFLMICHOU ',SIZE(GFLMICHOU),SHAPE(GFLMICHOU)
GFLMICHOU(:,:,:,:)=123.456
```

where the '3' in the first sentence refers to the amount of 3D fields you need for your extra output. If set to 3, you can e.g. put 2 3D fields and 61 2D fields or 3 3D fields in GFLMICHOU.
In src/arp/adiab/cpg.F90 we can fill GFLMICHOU with the data we need as output. First we add 'i' as an integer at line 603:

```
INTEGER(KIND=JPIM) :: IEND, IENDC, IPCT, IST, ISTC,i
```

We need to update the argument list of mf_phys whit the variables we need, and declare these variables. In section 4.4.2 we store the variables we want in the GFLMICHOU by

```
DO I=IST,IEND
 GFLMICHOU(I,9,3,IBL)=ZZPLCL(I,3)
ENDDO
```

In scr/arp/dia/wrgridua.F90 the extra output needs to become identifiable and written to the array where all output is written in. First we replace line 8 (USE YOMGFL   , ONLY : GFL) with:

```
USE YOMGFL   , ONLY : GFL      ,GFLMICHOU
USE YOMLUN   , ONLY : NULOUT
```

Then we add the following lines in section 3 after line 137 ['DEALLOCATE(ZGPFIELDS)'], where again the '3' refers to the amount of 3D fields you have declared in susc2b.F90.

```
IGPFIELDS=3*NFLEVG susc2b.F90
ALLOCATE(CLPREF(IGPFIELDS),ILEV(IGPFIELDS),CLSUFF(IGPFIELDS))
DO JGFL=1,3
  IOFF=(JGFL-1)*NFLEVG
  DO JLEV=1,NFLEVG
    CLPREF(IOFF+JLEV)='T   '
    ILEV(IOFF+JLEV)=JLEV
    CLSUFF(IOFF+JLEV)=YGFLC(JGFL)%CNAME(1:12)
  ENDDO
  WRITE(NULOUT,*)'YGFLC(JGFL)%CNAME(1:12) ',YGFLC(JGFL)%CNAME(1:12)
ENDDO

!JB Additional field
IGGP=3*NFLEVG
ALLOCATE(ZGPFIELDS(NGPTOT,IGGP))
DO JKGLO=1,NGPTOT,NPROMA
  IBL=(JKGLO-1)/NPROMA+1
  IST=1
  IEND=MIN(NPROMA,NGPTOT-JKGLO+1)
  IGFL=0
  DO JGFL=1,3
    IGFL=IGFL+1
    IOFF=(IGFL-1)*NFLEVG
    DO JLEV=1,NFLEVG
      DO JROF=IST,IEND
        ZGPFIELDS(JROF+JKGLO-1,IOFF+JLEV)=GFLMICHOU(JROF,JLEV,JGFL,IBL)
      ENDDO
    ENDDO
  ENDDO
ENDDO
```

In the first part the level type and name to identify the extra output field is defined. Here we use names of fields which are not used currently.

Finally, to make sure the extra output fields are also written to the GRIB files we need to check if the name of the variable and level type is defined in *src/util/gl/inc/trans_tab.h*. If not, then you can add them to the list.

Appendix B

In this appendix I will describe the changes in the code for the different perturbations. The perturbations with only changes in config_exp.h are excluded. Note that we have used cycle 36h1.4, thus if using an other cycle the line numbers can be different.

Runs:	15TOP / NOTOP
Location + routine:	src/arp/phys_dmn/vdfhghtnhl.F90
Line nr.:	300
Original:	ZCLDDEPTHDP = 4000._JPRB
Modification 15TOP:	ZCLDDEPTHDP = 1500.JPRB
Modification NOTOP:	ZCLDDEPTHDP = 100000.JPRB

Run:	NOMF
Location + routine:	nam/namelist_forecast
Line nr.:	44
Original:	LMFSHAL=.TRUE.,
Modification:	LMFSHAL=.FALSE.,
Added:	LMFSHAL=.FALSE.,

Runs:	ENTR_HIGH / ENTR_LOW
Location + routine:	src/arp/phys_dmn/vdfparcelhl.F90
Inserted after line nr.:	337 - ZEPS_LCL = min(0.05_JPRB,ZEPS_LCL)
Added (ENTR_HIGH):	ZEPS_LCL=0.05
Added (ENTR_LOW):	ZEPS_LCL=0.0005

Runs:	ML_HIGH / ML_LOW
Location + routine:	src/mpa/turb/internals/bl89.f90
Inserted after line nr.:	251 – ZLM(J1D,JK)=Z2SQRT2*ZLWORK1/(ZLWORK....
Added (ML_HIGH):	ZLM(J1D,JK) = 2.*ZLM(J1D,JK)
Added (ML_LOW):	ZLM(J1D,JK) = 0.5*ZLM(J1D,JK)

Runs:	GAMMA2 / GAMMA05
Location + routine:	src/mpa/micro/internals/ini_rain_ice.f90
Line nr.:	330
Original:	XNUR = 1.0
Modification (GAMMA2):	XNUR = 2.0
Modification (GAMMA05):	XNUR = 0.5

Runs:	SNOW
Location + routine:	src/mpa/micro/internals/ini_rain_ice.f90
Line nr.:	274
Original:	XCG = 124.
Modification:	XCG = 31.

Runs:	IP x 2 / IP x .5
Location + routine:	src/mpa/micro/internals/ini_rain_ice.f90

Line nr.: 213
Original XCCR = 8.E6
Modification (NCCDL): XCCR = 16.E6
Modification (NCCDS): XCCR = 4.E6

Runs: HAIL
Location + routine: src/mpa/micro/internals/ini_rain_ice.f90
Line nr.: 272-275
Original: XAG = 19.6
XBG = 2.8
XCG = 124.
XDG = 0.66
Modification: XAG = 470.
XBG = 3.0
XCG = 207.
XDG = 0.64

Runs: EVAP_HIGH / EVAP_LOW
Location + routine: src/mpa/micro/internals/rain_ice.f90
Added after line nr.: 1932 - (X0EVAR*ZLBDAR(:)**XEX0EVAR+X1.....
Added (EVAP_HIGH): ZZW(:) = MIN(ZRRS(:),2.0 * ZZW(:))
Added (EVAP_LOW): ZZW(:) = MIN(ZRRS(:),0.5 * ZZW(:))

Runs: NC x 3 / NC x .33
Location + routine: src/mpa/micro/internals/ini_rain_ice.f90
Line nr.: 393
Original: XCONC_LAND=3E8
Modification (NCS): XCONC_LAND=1E8
Modification (NCL): XCONC_LAND=9E8

Runs: IP x 2 / IP x .5
Location + routine: src/mpa/micro/internals/ini_rain_ice.f90
Line nr.: 330
Original: XNUR = 1.
Modification (IP x .5): XNUR = 0.5
Modification (IP x 2): XNUR = 2.0

Run: NOTOP + EVAP LCL
Location + routine: src/arp/phys_dmn/vdfhghtnhl.F90
Original (line 858-860):

```
ZUPFLXL(JL,JK,JD) = ZUPFLXL(JL,JK,JD) - ZPEVAPUP * ZDZRHO * ZFAC
ZUPFLXN(JL,JK,JD) = ZUPFLXN(JL,JK,JD) - ZPEVAPUP * ZDZRHO * (1._JPRB - ZFAC)
ZUPFLXL(JL,JK,JD) = MAX(0._JPRB,ZUPFLXL(JL,JK,JD))
```

Replace line 858-860 by (note a relative smooth increase of evaporation around LCL):

```
IF (JK.EQ.KPLCL(JL,3)-1) THEN
        ZUPFLXL(JL,JK,JD) = ZUPFLXL(JL,JK,JD) - ( ZPEVAPUP * ZDZRHO * ZFAC ) * 0.33_JPRB
        ZUPFLXN(JL,JK,JD) = ZUPFLXN(JL,JK,JD) - ( ZPEVAPUP * ZDZRHO * (1._JPRB - ZFAC) ) * 0.33_JPRB
ENDIF
IF (JK.EQ.KPLCL(JL,3)) THEN
        ZUPFLXL(JL,JK,JD) = ZUPFLXL(JL,JK,JD) - ( ZPEVAPUP * ZDZRHO * ZFAC ) * 0.67_JPRB
```

```
      ZUPFLXN(JL,JK,JD) = ZUPFLXN(JL,JK,JD) - ( ZPEVAPUP * ZDZRHO * (1._JPRB - ZFAC) ) * 0.67_JPRB
ENDIF
IF (JK.GT.KPLCL(JL,3)) THEN
      ZUPFLXL(JL,JK,JD) = ZUPFLXL(JL,JK,JD) - ZPEVAPUP * ZDZRHO * ZFAC
      ZUPFLXN(JL,JK,JD) = ZUPFLXN(JL,JK,JD) - ZPEVAPUP * ZDZRHO * (1._JPRB - ZFAC)
ENDIF
ZUPFLXL(JL,JK,JD) = MAX(0._JPRB,ZUPFLXL(JL,JK,JD))
```

Appendix C

In this appendix I will describe the bug (and fix) in EDMF_m, which is present in cycle 36h1.4. and results in reproducibility problems.

Three variables, that is *ZMU*, *ZB* and *ZBUOYRED*, in routine vdfparcelhl.F90 need to become and array of length KLON. Therefore in declaring the variables (line 176/177) *KLON* needs to be added (e.g. *ZMU(KLON)* instead of *ZMU*). Everywhere where these variables are used needs a *(JL)* added (e.g. *ZMU(JL)* instead of *ZMU*). In this way the correct values are used after the compilation process has split up the domain (also in the vertical) into different nodes. A new routine of vdfparcelhl.F90 with the bug fix can be found on twiki (http://twiki.knmi.nl/twiki/bin/view/Harmonie/WebHome).

Appendix D

Frequency bias index (FBI)

The FBI (also commonly referred to as 'bias') treats precipitation as a binary event. It counts the number of hits (event forecasted and observed – a), misses (even observed, not forecasted – c) and false alarms (event forecasted, not observed). Figure D1 illustrates this further. The FBI is then calculated as $FBI = a + b / a + c$, or i.e. *total forecasted yes / total observed yes.* The values range between 0 and infinity, where 1 indicates a perfect score. Note that a perfect score can be achieved by only hits, or also by the same amount of misses and false alarms without any hit. The FBI therefore does not say something about accuracy of the forecasted precipitation, but more about the frequency of forecasted precipitation events that are greater than a certain threshold. It therefore answers the question '*How did the forecast frequency of "yes" events compare to the observed frequency of "yes" events?'*. A FBI > 1 occurs if the event is overforecasted, and a FBI < 1 occurs if the event is underforecasted.

Equitable threat score (ETS)

The ETS, as FBI, treats precipitation as a binary event. It also counts the number of hits (a), misses (c) and false alarms (b), but is calculated as: $ETS = (a - a_r) / (a + b + c - a_r)$, where a_r is the 'hits by chance' (a_r = (a + b + c +d) / total sample size). The ETS is thus more aimed at the accuracy of the forecast, where the score is corrected for the hits generates by chance. The ETS therefore answers the question '*How well did the forecast "yes" events correspond to the observed "yes" events (accounting for hits due to chance)?*'. The score of an ETS can vary between -1/3 and 1, where 0 indicates no skill, and 1 is a perfect score.

Event forecast	Event observed		
	Yes	No	Marginal total
Yes	a	b	a + b
No	c	d	c + d
Marginal total	a + c	b + d	a + b + c + d =n

Figure D1: Description of deterministic verification score, source: http://www.eumetcal.org

Source: http://www.cawcr.gov.au/projects/verification/ (visited 5 September, 2012)

Appendix E

Currently, a persistent problem within Harmonie is the formation of fog fields over the North Sea when these are not observed. In case 1 such a fog field is also present (and not in observations). This allows for a closer look of the influence of the mixing length, as it is hypothesized that a too small cloud top entrainment could be the reason that the fog fields aren't removed (pers. comm. Wim de Rooy). A larger mixing length will increase the vertical mixing, thus also the cloud top entrainment. Figure E1 (left) shows the low cloud cover of ML x 2 at 00 and 12 UTC (July 10 – 2010). The fog field is clearly visible at 00 UTC (thus same as initial field). The enhanced mixing does remove the fog field partly (compared to REF – not shown), but at 12:00 UTC there is still a large fog field present over the North-Sea. If the data assimilation is run with the enhanced mixing then the fog field is not present anymore over the North Sea (fig E1 – right). This indicates the the fog field is very sensitive to extra turbulence.

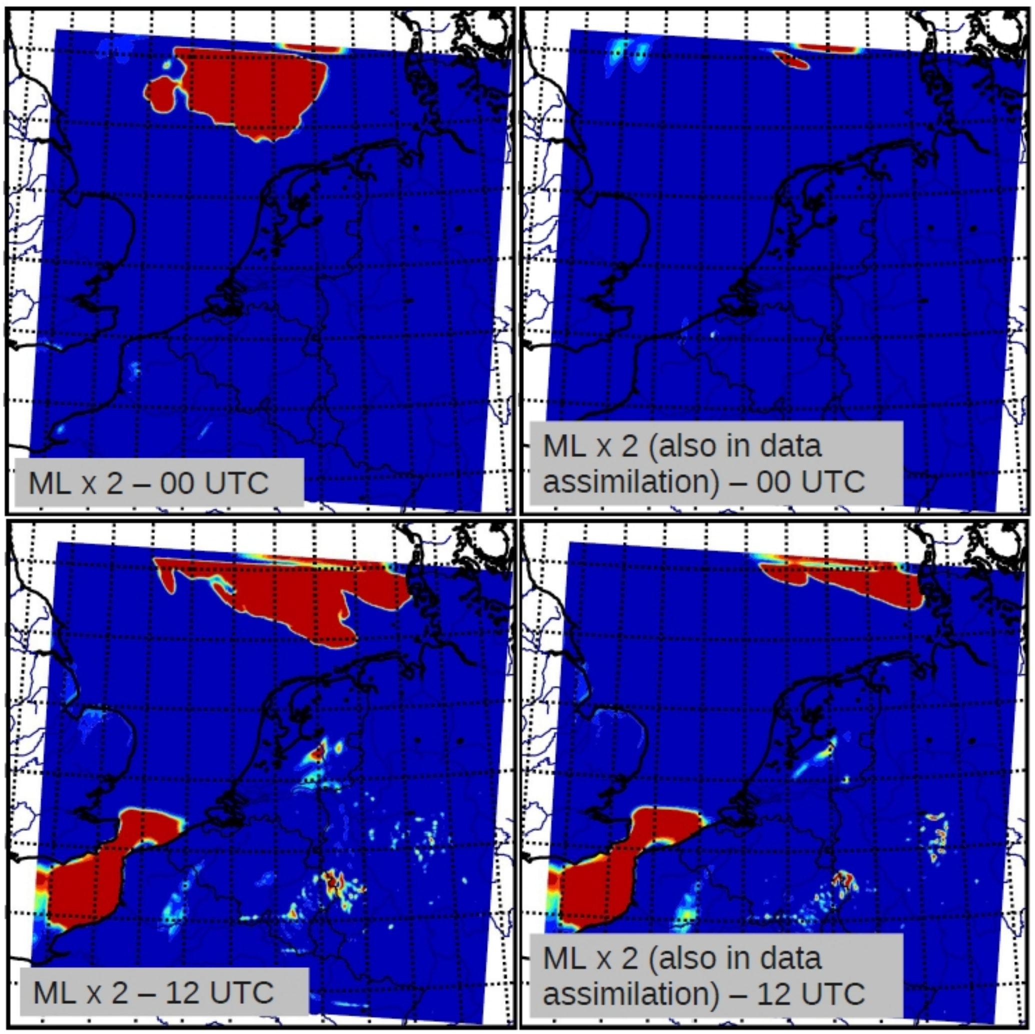

Figure E1: Low cloud cover of ML x 2 with standard warm start (left) and a warm start with a doubled mixing length in the physics (right), on times 00 and 12 UTC on 10 July 2010.

10. Literature

Belamari S, Pirani A, 2007: Validation of the optimal heat and momentum fluxes using the ORCA2-LIM global ocean–ice model. Marine environment and security for the european areaintegrated project (MERSEA IP), deliverable D4.1.3, p 88.

Bougeault, P. and P. Lacarrère, 1989: Parameterization of orography-induced turbulence in a mesobeta-scale model. Mon. Wea. Rev.,117, 1872–1890.

Bubnová, Radmila, Gwenaëlle Hello, Pierre Bénard, Jean-François Geleyn, 1995: Integration of the Fully Elastic Equations Cast in the Hydrostatic Pressure Terrain-Following Coordinate in the Framework of the ARPEGE/Aladin NWP System. Mon. Wea. Rev., 123, 515–535.

Cuxart et al. 2000: A turbulence scheme allowing for mesoscale and large eddy simulations, Quart.J.Roy.Met.Soc. 126,1-30.

Davidson, B., 1968: The Barbados Oceanographic and Meteorological Experiment. Bull. Amer. Meteor. Soc., 49, 928–934.

Gebhardt, C., S. E. Theis, P. Krahe, V. Renner, 2008: Experimental ensemble forecasts of precipitation based on a convection-resolving model. Atmos. Sci. Lett., 9 (2008), pp. 67–72.

Gebhardt, C., S. E. Theis, M. Paulat, and Z. Ben Bouallègue, 2010: Uncertainties in COSMO-DE precipitation forecasts introduced by model perturbations and variations of lateral boundaries. Atmos. Res., 100, 168–177.

Grant, A. L. M., 2001: Cloud-base fluuxes in the cumulus-capped boundary layer. Quart. J. Roy. Meteor. Soc., 127, 407–422.

Hohenegger, C. and C. Schär, 2007: Atmospheric predictability at synoptic versus cloud-resolving scales. Bulletin American Meteorol. Soc., 88 (11), 1783-1793.

Kain, J. S. and J. M. Fritsch. 1990. A one-dimensional entraining/detraining plume model and its application in convective parameterization. J. Atmos. Sci. 47:2784–2802.

Kain, J.S., and J.M. Fritsch, 1993: Convective parameterization for mesoscale models: The Kain-Fritsch scheme. The representation of cumulus convection in numerical models. Meteor. Monogr., No. 24, Amer. Meteor. Soc., 165-170.

Kessler, E., 1969: On distribution and continuity of water substance in atmospheric circulations. American Meteorological Society, Mereorol. Monogr., 10:32, 84.

Knievel, J. C., and R. H. Johnson, 1998: Pressure transients within MCS mesohighs and wake lows. Mon. Wea. Rev., 126, 1907–1930.

Knupp, K. R., and W. R. Cotton (1985), Convective cloud downdraft structure: An interpretive survey, Rev. Geophys., 23(2), 183–215

Leutbecher, M. and T.N. Palmer, 2008: Ensemble forecasting. Journal of Computational Physics, Volume 227, Issue 7, 3515-3539.

Lewis, John M., 2005: Roots of Ensemble Forecasting. Mon. Wea. Rev., 133, 1865–1885.

Mass, Clifford F., David Ovens, Ken Westrick, Brian A. Colle, 2002: Does Increasing Horizontal Resolution Produce More Skillful Forecasts?. Bull. Amer. Meteor. Soc., 83, 407–430.

Masson, 2000: A physically-based scheme for the urban energy budget in atmospheric models. Boundary Layer Meteorology, in press.

Le Moigne, Ed., 2009: SURFEX scientific documentation. Centre du Groupe de Me´te´orologie a` Moyenne Echelle Tech. Note 87, 211 pp

Morrison, H., Thompson, G., and Tatarskii, V, 2009.: Impact of cloud microphysics on the development of trailing stratiform precipitation in a simulated squall line: Comparison of one and two-moment schemes, Mon. Weather Rev., 137, 991–1006.

Neggers, Roel A. J., Martin Köhler, Anton C. M. Beljaars, 2009: A Dual Mass Flux Framework for Boundary Layer Convection. Part I: Transport. J. Atmos. Sci., 66, 1465–1487.

Noilhan, J., and S. Planton, 1989: A simple parameterization of land surface processes for meteorological models. Mon. Wea. Rev., 117, 536-549.

Palmer, T. N., Molteni, F., Mureau, R., Buizza, R., Chapelet, P. and Tribbia, J. (1993). Ensemble Prediction. In Proc. of the ECMWF Seminar on Validation of Models over Europe: Vol. 1, pp. 21–66, 7–11 September 1992, Reading, UK.

Pergaud, J., V. Masson, S. Malardel, F. Couvreux, 2009: A parameterization of dry thermalsand shallow cumuli for mesoscale numerical weather prediction. Bound. Layer. Meteor.,132, 83-106.

Pinty, J-P., and P. Jabouille, 1998: A mixed-phase cloud parameterization for use in mesoscale non-hydrostatic model: Simulations of a squall line and of orographic precipitations. Preprints,Conf. on Cloud Physics, Everett, WA, Amer. Meteor. Soc., 217–220.

Rauber, Robert M., and Coauthors, 2007: In the Driver's Seat: Rico and Education. Bull. Amer. Meteor. Soc., 88, 1929–1937.

Richard, E., N. Asencio, R. Benoit, A. Buzzi, R. Ferretti, P. Malguzzi, S. Serafin, G. Zängl, and J.-F. Georgis, 2002: Intercomparison of the simulated precipitation fields of the MAP/IOP2b with different high-resolution models. Proc. 10th Conf. on Mountain Meteorology and MAP Meeting, Park City, UT, Amer. Meteor. Soc., 167–170.

de Rooy, Wim C., A. Pier Siebesma, 2008: A Simple Parameterization for Detrainment in Shallow Cumulus. Mon. Wea. Rev., 136, 560–576.

de Rooy, W., P. Bechtold, K. Froehlich, C. Hohenegger, H. J. J. Jonker, D. Mironov, A. P. Siebesma, J. Teixeira, and J. Yano (2012), Entrainment and detrainment in cumulus convection: an overview, Quart. J. Roy. Meteorol. Soc.

Schaefer, J.T., 1990. The critical success index as an indicator of warning skill. Wea. Forecasting 5, 570–575.

Seity, Y., P. Brousseau, S. Malardel, G. Hello, P. Bénard, F. Bouttier, C. Lac, V. Masson, 2011: The AROME-France Convective-Scale Operational Model. Mon. Wea. Rev., 139, 976–991.

Smith, J.A., Hui, E., Steiner, M., Baeck, M.L., Krajewski, W.F., Ntelekos, A.A., 2009: Variability of rainfall rate and raindrop size distributions in heavy rain. Water Resources Research 45, p. W04430(12).

Stevens B. and A. Seifert, 2008: Understanding macrophysical outcomes of microphysical choices in simulations of shallow cumulus convection, J. Met. Soc. Japan , 86A , 143_162.

Wilks, D.S., 1995: Statistical Methods in the Atmospheric Sciences. Academic Press, New York. 467 pp.

Wisse, J. S. P. and Vilà-Guerau de Arellano, J., 2004: Analysis of the role of the planetary boundary layer schemes during a severe convective storm, Ann. Geophys., 22, 1861-1874.

A complete list of all KNMI-publications (1854 – present) can be found on our website

www.knmi.nl/knmi-library/knmipub_en.html

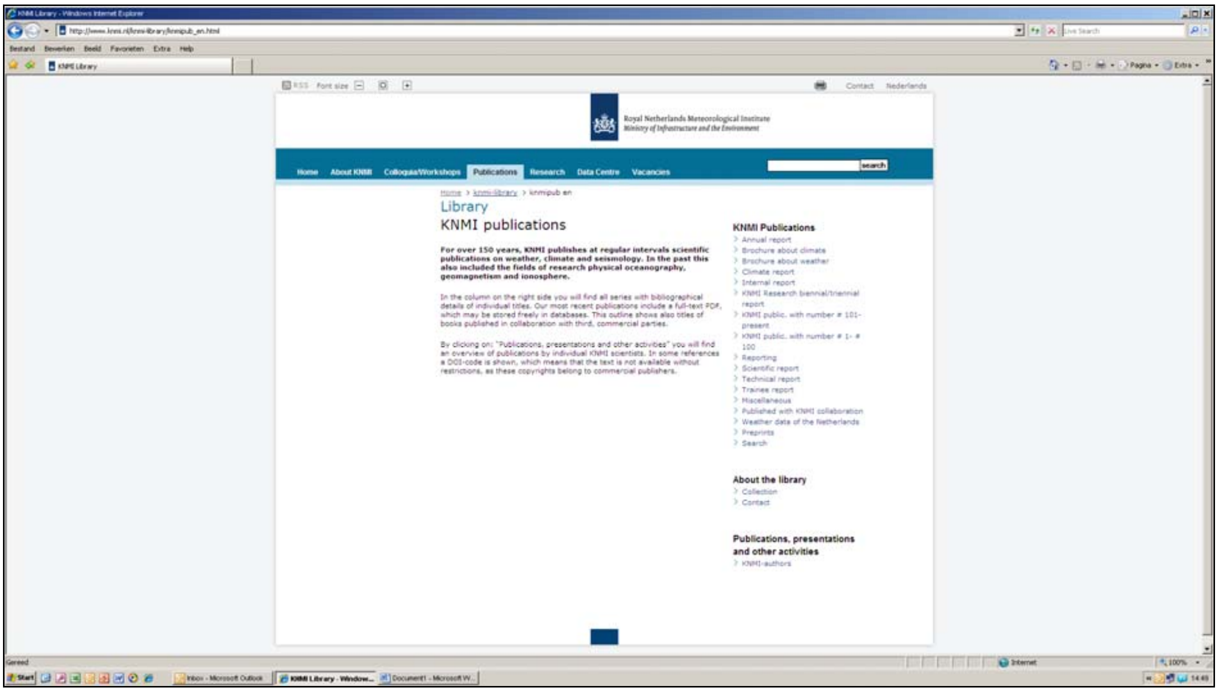

The most recent reports are available as a PDF on this site.